EXPERIMENTAL STUDY OF HEAT TRANSFER COEFFICIENT OF NANOFLUID FLOW THROUGH A PLAIN TUBE

AZRUL AZAM BIN NIZARUDIN

BACHELOR OF ENGINEERING

UNIVERSITI MALAYSIA PAHANG

2010

UNIVERSITI MALAYSIA PAHANG

BORANG PENGESAHAN STATUS TESIS♦

JUDUL: **EXPERIMENTAL STUDY OF HEAT TRANSFER COEFFICIENT OF NANOFLUID FLOW THROUGH A PLAIN TUBE**

SESI PENGAJIAN:___**2010/2011**_____

Saya _____**AZRUL AZAM BIN NIZARUDIN (850302-03-5139)**_____
(HURUF BESAR)

mengaku membenarkan tesis (Sarjana Muda/~~Sarjana~~ /~~Doktor Falsafah~~)* ini disimpan di Perpustakaan dengan syarat-syarat kegunaan seperti berikut:

1. Tesis adalah hakmilik Universiti Malaysia Pahang (UMP).
2. Perpustakaan dibenarkan membuat salinan untuk tujuan pengajian sahaja.
3. Perpustakaan dibenarkan membuat salinan tesis ini sebagai bahan pertukaran antara institusi pengajian tinggi.
4. **Sila tandakan (√)

	SULIT	(Mengandungi maklumat yang berdarjah keselamatan atau kepentingan Malaysia seperti yang termaktub di dalam AKTA RAHSIA RASMI 1972)
	TERHAD	(Mengandungi maklumat TERHAD yang telah ditentukan oleh organisasi/badan di mana penyelidikan dijalankan)
√	TIDAK TERHAD	

Disahkan oleh:

_____   _____
(TANDATANGAN PENULIS)   (TANDATANGAN PENYELIA)

Alamat Tetap:

NO. 189, RPT KESEDAR SG. TERAH   **WAN AZMI BIN WAN HAMZAH**
18300 GUA MUSANG   (Nama Penyelia)
KELANTAN

Tarikh: **6 DISEMBER 2010**   Tarikh: **6 DISEMBER 2010**

CATATAN: * Potong yang tidak berkenaan.
** Jika tesis ini SULIT atau TERHAD, sila lampirkan surat daripada pihak berkuasa/organisasi berkenaan dengan menyatakan sekali tempoh tesis ini perlu dikelaskan sebagai atau TERHAD.
♦ Tesis dimaksudkan sebagai tesis bagi Ijazah doktor Falsafah dan Sarjana secara Penyelidikan, atau disertasi bagi pengajian secara kerja kursus dan penyelidikan, atau Laporan Projek Sarjana Muda (PSM).

UNIVERSITI MALAYSIA PAHANG
FACULTY OF MECHANICAL ENGINEERING

I certify that the project entitled "*Experimental Study of Heat Transfer Coefficient of Nanofluid Flow through a Plain Tube*" is written by *Azrul Azam bin Nizarudin*. I have examined the final copy of this project and in our opinion; it is fully adequate in terms of scope and quality for the award of the degree of Bachelor of Engineering. I herewith recommend that it be accepted in partial fulfillment of the requirements for the degree of Bachelor of Mechanical Engineering.

Examiner   Signature

EXPERIMENTAL STUDY OF HEAT TRANSFER COEFFICIENT OF
NANOFLUIDS FLOW THROUGH A PLAIN TUBE

AZRUL AZAM BIN NIZARUDIN

Report submitted in partial fulfillment of the requirements
for the award of the degree of
Bachelor of Mechanical Engineering

Faculty of Mechanical Engineering
UNIVERSITI MALAYSIA PAHANG

DECEMBER 2010

SUPERVISOR'S DECLARATION

I hereby declare that I have checked this project and in my opinion, this project is adequate in terms of scope and quality for the award of the degree of Bachelor of Mechanical Engineering.

Signature

Name of Supervisor: WAN AZMI BIN WAN HAMZAH

Position: LECTURER

Date:

STUDENT'S DECLARATION

I hereby declare that the work in this thesis is my own except for quotations and summaries which have been duly acknowledged. The thesis has not been accepted for any degree and is not concurrently submitted for award of other degree.

Signature
Name: AZRUL AZAM BIN NIZARUDIN
ID Number: MA08018
Date:

**Dedicated to my beloved parents for their everlasting love, guidance and support
in the whole journey of my life**

ACKNOWLEDGEMENTS

ABSTRACT

Heat transfer is one of the most important processes in many industrial. The inherently poor thermal performance of common fluids put a limitation and restricted in developing energy efficient heat transfer fluid. With a strong needed by industry in developing energy efficient, advance heat transfer fluid called nanofluid is introduced. Nanofluid is prepared by two step technique in this study by diluting Alumina nanoparticles with water at three different concentrations 0.02%, 0.10% and 0.50%. The heat transfer coefficient was investigated experimentally in a flow loop with a horizontal tube test section subjected to constant heat flux at a various flow rate ranges between Reynolds number 4,000 to 20,000. Initial experiments were conducted with pure water for experiment validation and accuracy. The experimental results, represented in Nusselt number (*Nu*) are compared to classical Gnielinski equation and Dittus-Boelter equation and observed that both equations are applicable in turbulent flow range for single phase fluid with considerable deviation was observed. Addition of the nanoparticles to the base fluid significantly increased their heat transfer coefficient and the maximum enhancement of 19.80% compared with pure water with 0.50% volume concentration and at Reynolds number 8,400 was observed in this study. However, increasing of small amount of volume concentrations in the small range studied in this work did not show much effect on heat transfer enhancement. Experimental result were compared with previous result in literature and numerical study and found consistent with considerable deviation observed.

ABSTRAK

Pemindahan haba adalah salah satu proses penting di dalam kebanyakan industri. Cecair biasa seperti air secara semulajadi mempunyai kadar pengaliran haba yang lemah dan sekaligus membataskan pembangunan untuk mencapai kadar yang efisyen dalam pemindahan haba. Dengan permintaan yang tinggi daripada industri untuk mencapai kadar yang efisyen dalam pemindahan haba ini, 'nanofluid' telah diperkenalkan. 'Nanofluids' ini disediakan dengan kaedah 'two step' teknik yang mana serbuk Alumina dicairkan dengan air kepada tiga kecairan yang berbeza iaitu 0.02%, 0.10% dan 0.50%. Pekali kadar pemindahan haba telah ditentukan melalui eksperimen di dalam salur paip yang diletakkan secara mendatar dan terdedah kepada kepanasan fluks yang malar pada kadar aliran yang berbeza dari nombor Reynolds 4,000 ke 20,000. Permulaan eksperimen telah menggunakan air sebagai untuk memastikan radas eksperimen berfungsi dengan baik dan mencapai ketepatan yang dibolehkan. Keputusan eksperimen yang diperoleh telah di persembahkan di dalam bentuk nombor Nusselt dan kemudiannya di bandingkan dengan persamaan klasik Gnielinski dan Dittus-Boelter mendapati kedua-dua persamaan ini boleh diguna pakai pada analisa aliran secara turbulen serta satu fasa dengan kadar perbezaan yang boleh diterima. Penambahan serbuk nano ke dalam bendalir asal menyebabkan peningkatan kadar pemindahan haba dan kadar maximum peningkatan kadar pemindahan haba 'nanofluid' adalah 19.80% pada kecairan 0.50% dan nombor Reynolds 8,400 telah direkodkan di dalam kajian ini. Walaubagaimanapun, penambahan kecairan 'nanofluid' yang sedikit didalam linkungan kajian ini tidak menunjukkan banyak perubahan terhadap peningkatan kadar pemindahan haba. Keputusan eksperimen ini telah dibandingkan dengan keputusan pengkaji sebelum ini serta kajian melalui kaedah matematik dan mendapati ianya konsisten dengan perbezaan yang boleh diterima direkodkan.

TABLE OF CONTENTS

CHAPTER 3   METHODOLOGY

CHAPTER 4   RESULTS AND DISCUSSION

LIST OF TABLES

LIST OF FIGURES

LIST OF SYMBOLS

D_i	Inner diameter of the tube, (m)
h	Convective heat transfer coefficient, ($W/m^2.K$)
k	Thermal conductivity, ($W/m.K$)
μ	Dynamic viscosity of the fluid, ($kg/m.s$)
ρ	Density of the fluid, (kg/m^3)
C_p	Specific heat, ($J/kg.K$)
L	Length of the tube, (m)
$\dot{m}$	Mass flow rate, (kg/s)
$\dot{Q}_{conv}$	Heat convection rate, ($Watt$)
$\dot{q}_s$	Heat Flux, (W/m^2)
f	Friction factor
Nu	Nusselt number
Re	Reynolds number
Pr	Prandtl number
ΔP	Pressure difference
T_b	Bulk fluid temperature, (^oC)
T_s	Surface temperature, (^oC)
T_w	Wall temperature, (^oC)
ΔT	Temperature difference
ε	Roughness size, (m)
g	Gravitational acceleration, (m/s^2)
$\emptyset$	Volume concentration of nanofluid
A_s	Surface area, (m^2)

A_c Cross sectional area, (m^2)

V_{avg} Average velocity, (m/s)

V Voltage, (Volt)

I Current, (Amphere)

nf Nanofluid

exp Experiment

W Water

Reg Regression

LIST OF ABBREVIATIONS

FIST   Fakulti Sains & Teknologi Industri

FKM   Fakulti Kejuruteraan Mekanikal

FYP   Final year project

HTC   Heat Transfer Coefficient

STD   Standard deviation

Al   Aluminum

Cu   Copper

Ag   Silver

Au   Gold

Al_2O_3 Aluminum Oxide/Alumina

CuO   Copper Oxide

TiO   Titanium Oxide

SiC   Silicon Carbide

SiN   Silicon Nitride

ZrO_2 Zirconia Oxide

CHAPTER 1

INTRODUCTION

1.1   PROJECT BACKGROUND

Heat transfer fluids, such as water, ethylene glycol and mineral oil play an important role in many industrial processes, including power generation, heating and cooling processes. These common fluids have poor heat transfer performance compared to those most solids (Eastman, 1997). The earlier studies to enhance heat transfer properties have done by Maxwell (1873), and used suspensions of millimeter or micrometer sized particles, which although showed some enhancement but some problems experienced such as poor suspension stability and channel clogging, extra pressure drop and erosion of pipeline. Although the solutions show better thermal performance compared to common heat transfer fluids, they are still not suitable for use as heat transfer fluids in practical applications. In 1995, Choi has been advanced the concept of nanofluids that showed substantial augmentation of heat transported in suspensions of copper or aluminum nanoparticles in water and other common liquids by dispersions of nanoparticles in liquids that are permanently suspended by Brownian motion. Nanofluid has been found to be an attractive heat transport fluids. It has exhibited a significant potential for heat transfer augmentation relative to the conventional pure fluids. It has been expected to be suitable for the engineering application without severe problems in pipeline and with little or no penalty in pressure drop. Here, attention to study a convective heat transfer coefficient of nanofluid is draw in term of enhancing the rate of heat transfer.

1.2   PROBLEM STATEMENT

Heat transfer is one of the most important processes in many industrial and consumer product. The inherently poor thermal performance of conventional fluids puts a limitation on heat transfer and restricted in developing energy efficient heat transfer fluids that are required for ultrahigh performance cooling. With increasing global competition, industries have a strong need to develop advanced heat transfer fluids with significantly higher thermal performance than are presently available. Therefore, scientists and engineers have made a great effort to break this fundamental limit by dispersing metallic and non-metallic particles in liquids. This concept of new kind of fluid called 'nanofluid' has introduced by Choi, (1995).

In order to commercialize this new kind of fluid, many researchers have attempted study on heat transfer performance and flow characteristic of this fluid. From the previous publish report of nanofluid, they have claimed that nanofluid thermal properties is higher than base fluid such as water, mineral oil and ethylene glycol. Nanofluid technologies have offer a great potential for further development of high performance, compact and cost effective cooling to utilizing in industrial applications.

Thus, studies of heat transfer behavior for nanofluids are essential in providing authentification result that have found by previous researchers.

1.3   OBJECTIVES OF STUDY

In this study, there are several objectives need to fulfill as described below;

i.   To estimate the heat transfer coefficient (HTC) of nanofluid flowing through a plain tube.

ii. To validate result obtain from experiment by comparing with the previous result in literature and numerical method.

1.4   SCOPE OF THE STUDY

There are several scopes included in this research as follow:

i.   Alumina (Al_2O_3) nanofluids dilute by water is flow under fully developed turbulent region.

ii.   Nanofluids flow through a plain tube with constant heat flux boundary conditions.

iii.   Using Al_2O_3/Water Nanofluids with volume concentration 0.02%, 0.05% and 0.5%

iv.   Evaluate HTC under turbulent region with Reynolds number ranged between 4,000 and 20,000.

1.5   SIGNIFICANCE OF STUDY

Heat transfer coefficient (HTC) is a better indicator in evaluate of thermal performance of the fluid. Thus, it is really important to know how to get the value of HTC since it is not a property of the fluid and it is experimentally determine parameter whose value depends on all variables influencing convection such as the surface geometry, the nature of fluids motion, and the properties of the fluid and bulk fluid velocity.

Volume concentration, flow condition, constant heat flux and surface temperature of the wall tube is played a big role in nanofluid thermal performance, study of the HTC effect with varies parameter will give a guideline to produce nanofluid with ideal composition.

1.6   PROJECT FLOW CHART

Figure 1.1 shows the process flow of the project with step by step start from beginning of the project until the end.
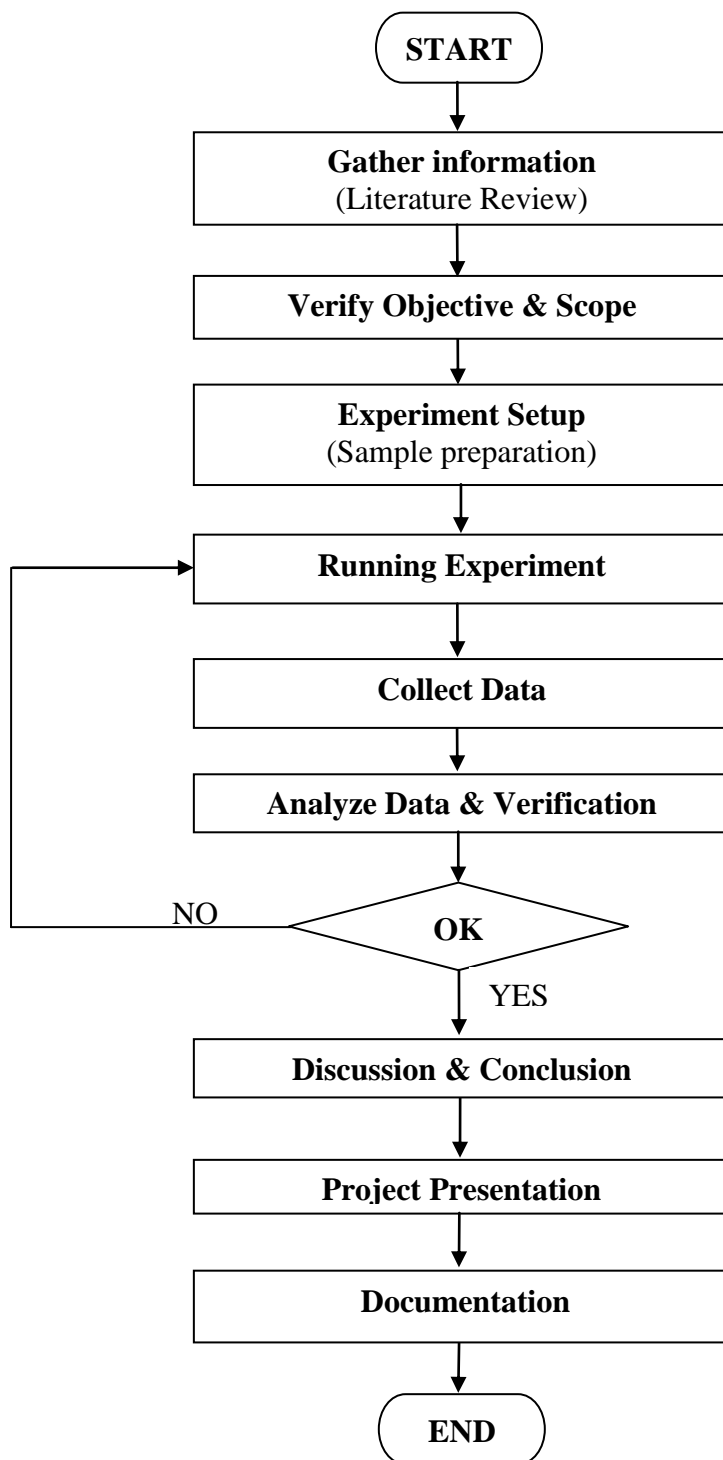
Figure 1.1: Project Flow Chart

1.7   CONCLUSION

Experimental study of convective heat transfer of Alumina (Al_2O_3) Nanofluids dilute by water used in this study with three varies concentration of 0.02%, 0.05% and 0.5%. This study is to determine the heat transfer coefficient of nanofluid with different volume concentration flowing through a plain tube with fully develops turbulent flow. The test section is subjected to the constant heat flux along the plain tube. Result obtained from this study is validating with previous research result and numerical study result and convenience as an indicator for choosing a cooling fluids.

CHAPTER 2

LITERATURE REVIEW

2.1   INTRODUCTION

Nanofluid has been found to be an attractive heat transport fluids. It has exhibited a significant potential for heat transfer augmentation relative to the conventional pure fluids. It has been expected to be suitable for the engineering application without severe problems in pipeline and with little or no penalty in pressure drop. Basically, this new kind of fluid are produced by dispersions of nanoparticles in water or other common liquids and permanently suspended by Brownian motion. In this chapter, the process of making nanofluid and the applications of nanofluids in industry will be explained. Then, some discussion on theory of heat transfer together with dimensionless parameter that are related to this study is organized chronologically to laid the groundwork for subsequent studies, including the present research effort. The review is detailed so that the present research effort can be properly tailored to add to the present body of literature as well as to justly the scope and direction of the present research effort. Finally, advantages and disadvantages of nanofluid have been explained at the end of this chapter.

2.2   HISTORY OF NANOFLUID

The process to produce advance fluids has done in the earlier 1981 when D.B. Tuckerman introduced microchannel technology. Four years later, Argonne National Laboratory starts program to develop advanced fluids. Various initiatives had done from micro to nano sized particles after Choi realize of Argonne capability for nanoparticle production. Choi in 1995 has been advanced the concept of nanofluid that showed substantial augmentation of heat transported in suspensions of copper or aluminum nanoparticles in water and other common liquids. For the past decade, research institutions worldwide have established research group on nanofluid and in shortly, nanofluids become a new field of scientific research that has grown enormously in the past few years. Despite recent advances, such as discoveries of unexpected thermal properties, proposed new mechanisms, and unconventional models proposed, the mysteries of nanofluids are unsolved. Nanofluids are an interdisciplinary ensemble of several fields of science and technology. Much work is necessary in every area of nanofluids, from fundamentals to formulation to large-scale production. Table 2.1 has summarized the history of the emergence of nanofluid as a new field of inquiry.

Table 2.1: Timeline of emergence of nanofluids

Years	Descriptions
1981	D.B. Tuckerman introduces microchannel technology
1985	Argonne National Laboratory start program to develop advance fluids
1991	Choi develops a microchannel heat exchanger for Advance Photon Source at Argonne.
1992	Funding cut for Argonne advance fluids program. Choi turn attention from micro to nano.
1993	Choi learn of Argonne capability for nanoparticle production
1995	Choi present a seminar paper of the concept of nanofluids at ASME Winter Annual Meeating, San Francisco, CA, Nov. 12-17
1999	Choi's group publishes the firs SCI article on nanofluid
2001	Choi's group publishes two papers in Applied Physics Letters
2007	The first single-theme conference on nanofluids was held. The first book on nanofluids, *Nanofluids: Science and Technology*, is published by Wiley

2.3   NANOFLUID PREPARATION

Materials for base fluids and nanoparticles are diverse. Stable and highly conductive nanofluids are produced by one and two-step production methods. Both approaches to creating nanoparticle suspensions suffer from agglomeration of nanoparticles, which is a key issue in all technology involving nanopowders. Therefore, synthesis and suspension of nearly non-agglomerated or monodispersed nanoparticles in liquids is significant enhancement in the thermal properties of nanofluids.

2.3.1   Materials for Nanoparticles and Fluids

Modern nanotechnology has enabled the production of metallic or nonmetallic nanoparticles with average crystallite sizes below 100 nm. The mechanical, optical, electrical, magnetic, and thermal properties of nanoparticles are superior to those of conventional bulk materials with coarse grain structures. Consequently, research and development investigation of nano-phase materials has drawn considerable attention from both material scientists and engineers (Duncan and Rouvray, 1989).

Nanoparticles used in nanofluids have been made of various materials, such as oxide ceramics (Al_2O_3, CuO), nitride ceramics (A_lN, SiN), carbide ceramics (SiC, TiC), metals (Cu, Ag, Au), semiconductors (TiO_2, SiC), carbon nanotubes, and composite materials such as alloyed nanoparticles $Al_{70}Cu_{30}$ or nanoparticle core polymer shell composites. In addition to nonmetallic, metallic, and other materials for nanoparticles, completely new materials and structures, such as materials "doped" with molecules in their solid liquid interface structure, may also have desirable characteristics. The common liquid normally used as a base fluid in nanofluid such as water, mineral oil and ethylene glycol.

2.3.2   Method of Nanoparticles Manufacture

The current processes for making metal nanoparticles is Inert Gas Condensation (IGC), mechanical milling, chemical precipitation, thermal spray, and spray pyrolysis. Most recently, Chopkar, et al. (2006) produced alloyed nanoparticles $Al_{70}Cu_{30}$ using ball milling. In ball milling, balls impart a lot of energy to slurry of powder, and in most

cases some chemicals are used to cause physical and chemical changes. These nano sized materials are most commonly produced in the form of powders. In powder form, nanoparticles are dispersed in aqueous or organic host liquids for specific applications.

2.3.3 Dispersion Nanoparticles in Liquids

Nanofluids have been produced by two techniques which is single step and two step techniques. The single step techniques is simultaneously makes and disperses the nanoparticles directly into the base fluid and two step techniques starts with nanoparticles produced by one of the physical or chemical systhesis techniques and proceeds to disperse them into a base fluid.

Most of the nanofluids containing oxide nanoparticles and carbon nanotubes are produces by the two step process. Moreover, an ultrasonic vibrator or magnetic stirrer was used to sonicate the solution continuously for approximately tenth hours in order to break down agglomeration of the nanoparticles.

2.4 APPLICATION OF NANOFLUID

Heat transfer fluids play an important role for cooling applications in many industries including manufacturing, transportation, energy, and electronics. Nanofluids can be used to improve heat transfer and energy efficiency in a variety of thermal system, including the important applications of vehicle cooling. Some of the application of nanofluids will be discuss in the next sub chapter.

2.4.1 Nanofluid for Cooling Applications

Developments in new technologies such as highly integrated microelectronic devices, higher power output engines, and reduction in applied cutting fluids continuously increase the thermal loads, which require advances in cooling capacity. Therefore, there is a needed for new and innovative heat transfer fluids to achieve better cooling performance.

Generally, conventional heat transfer fluids have poor heat transfer properties compared to solids. As shown in Table 2.2, most solids have orders of magnitude larger thermal conductivities than those of conventional heat transfer fluids. Therefore, fluids containing suspended solid particles are expected to display significant enhancement in thermal conductivities relative to conventional heat transfer fluids.

Table 2.2: Thermal Conductivity of Various Materials at Room Temperature

	Material	**Thermal Conductivity** (*W/m.K*)
Metallic	Silver	429
Solids	Copper	401
	Aluminum	237
Nonmetallic Solids	Diamond	3300
	Carbon nanotubes	3000
	Silicon	148
	Alumina (Al_2O_3)	40
Metallic liquids	Sodium at 644 K	72.3
Nonmetallic liquids	Water	0.613
	Ethylene glycol	0.253
	Engine oil	0.145

At 300K unless denoted

Source: Eastman et al. (1997)

In addition, normal coolant operating temperature can be increased since nanofluids have obtained a higher boiling point, which is desirable for maintaining single phase coolant flow. The results of nanofluids research are being applied to the cooling of automatic transmission with variable operating speeds conducted by Tzeng, et al. (2005) found the CuO nanofluids produced the lowest transmission temperatures both at high and low rotating speeds.

2.4.2 Nanofluid for Lubrication Applications

Solid lubricants are useful for conditions when conventional liquid lubricants are inadequate such as high temperature and extreme contact pressures. Their lubricating properties are attributed to a layered structure on the molecular level with weak bonding

between layers. Graphite and molybdenum disulfide (MoS_2) are the predominant materials used as solid lubricant. Other useful solid lubricants include boron nitride, tungsten disulfide, polytetrafluorethylene (PTFE), and etc.

In order to improve the tribological properties of lubricating oils, nanoparticle is dispersing into solid lubricants. Recent research has shown that lubricating oils with nanoparticles additives exhibit improved load-carrying capacity, anti-wear and friction-reduction properties. Xu, et. al. (1996) investigated tribological properties of the two-phase lubricant of paraffin oil and diamond nanoparticles, and the results showed that, under boundary lubricating conditions, this kind of two-phase lubricant possesses excellent load-carrying capacity, anti-wear and friction-reduction properties.

2.4.3   Biomedicine Applications

Nanofluids have many applications in the biomedical industry. For example, nanofluids are used to producing effective cooling around the surgical region and thereby enhancing the patient's chance of survival and reducing the risk of organ damage. In a contrasting application to cooling, nanofluids could be used to produce a higher temperature around tumors to kill cancerous cells without affecting nearby healthy cells (Jordan, et al., 1999).

2.4.4   Others Applications

There are unending situations where an increase in the heat transfer effectiveness can be beneficial to be the quality, quantity, and cost of product or process. In many of these situations, nanofluids are good candidates for accomplishing the enhancement in heat transfer performance. For example, nanofluids have potential application in buildings where increases in energy efficiency could be realized without increases in energy efficiency without increased pumping power. Such an application would save energy in as heating, ventilating and air conditioning system while providing environmental benefits. In the renewable energy industry, nanofluids could be employed to enhanced heat transfer from solar collectors to storage tanks and increase the energy

density. Nanofluid coolants also have potential application in major process industries, such as materials, chemical, food and drink, oil and gas, paper and printing, and textiles.

2.5   THEORY OF HEAT TRANSFER

Heat is defined as a form of energy that can be transferred from one system to another system as a result of temperature difference. Heat transfers is deals with determination of the rates of such energy transfers and always occur from the higher temperature to lower temperature and its stop when the two mediums reach the same temperature. Heat can be transferred in three different modes which are conduction, convection and radiation. All modes require the existence of a temperature difference, and all modes from the high temperature medium to a lower one. For nanofluids flowing through a plain tube, it considered internal flow and heat is transferred by convection mode since it is involved fluid as a medium of heat transfer.

2.5.1   Convection

Convection is mode of energy transfer between a solid surface and the adjacent liquid or gas that is in motion and it involves the combined effects of conduction and fluid motion. The faster liquid motion, the greater the convection heat transfers. Convection is strongly depends on the fluid properties such as dynamic viscosity, thermal conductivity, density, specific heat and fluid velocity.

Heat transfer process that involve change of phase of a fluid are also considered to be convection because of the fluid motion induced during the process, such as the rise of the vapor bubbles during boiling or the fall of the liquid droplets during condensations. The rate of heat transfer in the convection is observed to be proportional to the temperature difference and is expresses by Newton's law of cooling in Eq. 2.1.

$$\dot{Q}_{Conv} = hA_s\Delta T_{avg} = hA_s\left(T_s - T_\infty\right) \qquad (\text{W}) \qquad\qquad (2.1)$$

Where, h is convection heat transfer coefficient in W/m².$^{\text{o}}$C, A_s is surface area, T_s is surface temperature and T_∞ is ambient temperature.

The value of heat transfer coefficient h is not a property of the fluid and it is experimentally determine parameter whose value depends on all variables influencing convection such as the surface geometry, the nature of fluids motion, and the properties of the fluid and bulk fluid velocity. Typical value of h is given in Table 2.3.

Table 2.3: Typical Value of Convection Heat Transfer Coefficient

Type of Convection	h, W/m². º C
Free convection of gases	2 – 25
Free convection of liquids	10 – 1000
Forced convection of gases	25 – 250
Forced convection of liquids	50 – 20,000
Boiling and condensation	2500 – 100,000

Source: Cengel (2006)

Convection is divided by two ways which is forced convection and natural convection (free convection). Natural convection is occur in naturally without any motion in the air and due to the rise of the warmer air near the surface and the fall of the cooler air to fill its place. Forced convection will be explained on the next sub chapter.

2.5.2   Forced Convection

Forced convection is caused by fluid flow is force over the surface by external means such as pump, fan or blower. There are two main situations of forced convection which is external forced convection and internal forced convection. External forced convection normally occur when the fluid flow over a surface such as plate, a wire and pipe. However, internal forced convection occurs in pipe or duct. Internal forced convection will briefly explain on the next sub-chapter.

2.5.3 Internal Forced Convection

The terms pipe, duct and conduit are usually refer to the internal flows and descriptive phrase for pipes (circular cross section), duct (noncircular cross section), and tubes (is refer to smaller diameter size). Most of the fluids an especially liquid is transported in circular tubes since its can withstand large pressure differences between the inside and outside without undergoing significant distortion. Noncircular pipes are usually used in applications such as cooling and heating systems of building where the pressure difference is relatively small.

2.5.4 Average Velocity and Temperature

In internal flow, the fluid velocity in a tube changes from zero at the surface because of no-slip condition to maximum at the tube center as shown in Figure 2.1. Therefore, it is convenient to work with average velocity or mean velocity V_{avg}, which remains constant for incompressible flow when the cross sectional area of the tube is constant.

The value of average velocity is obtained from conservation of mass principle in Eq. 2.2.

$$\dot{m} = \rho V_{avg} A_c = \int_{A_c} \rho u(r) dA_c \qquad (2.2)$$
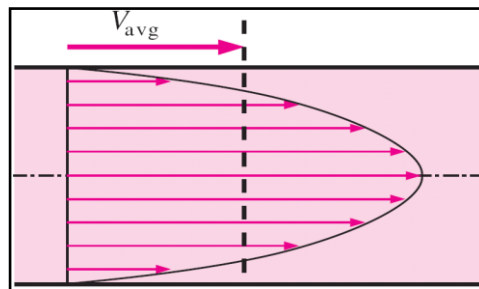
Figure 2.1: Average Velocity for Fully Develop Flow

Source: Cengel (2006)

2.5.5   The Entrance Region

The entrance region is very important in internal flow, we have to determine whether the flows inside the pipe or duct flow in fully develop or not. For example, fluid flows enter a circular pipe at a uniform velocity have a different velocity because of no-slip condition at wall of the pipe. Thus, velocity gradient have develops along the pipe and fluid layer in the contact with the surface of pipe come to a complete stop and causes the fluid particles in the adjacent layers to slow down gradually as a result of friction. The region of the flow in which the effects of the viscous shearing forces caused by the fluid viscosity are felt is called velocity boundary layer or boundary layer as shown in Figure 2.2.
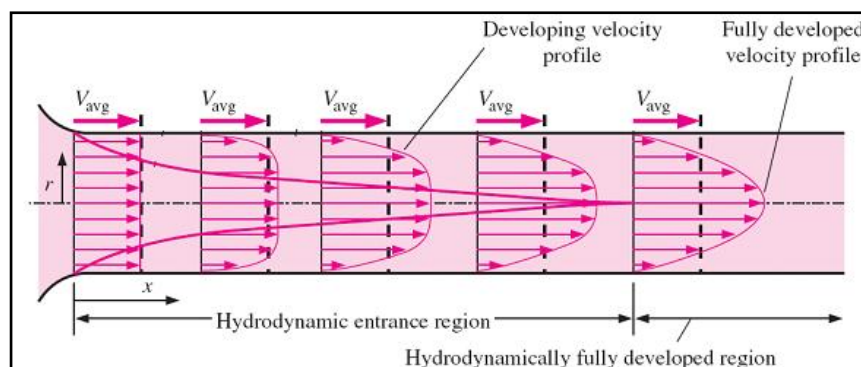
Figure 2.2: Boundary Layer for Entrance Region

Source: Cengel (2006)

However, fluid flow at uniform temperature entering a circular tube with surface at the different temperature and the fluid particles is in the layer in contact with surface of the tube. The thickness of the boundary layer also increases in the flow direction until the boundary layer reaches the tube center and thus fills the entire tube as shown in Figure 2.3.

The entry length is usually taken to be the distance from the tube entrance where the wall of shear stress reaches within about two percent of the fully develop value. For laminar flow, the hydrodynamic and thermal entry length can be obtained from

approximate equation by Kays and Crawford, (1993) and Shah and Bhati, (1987) in Eq. 2.3 and 2.4.

$$L_{h,laminar} \approx 0.05ReD \tag{2.3}$$

$$L_{t,laminar} \approx 0.05RePrD = PrL_{h,laminar} \tag{2.4}$$
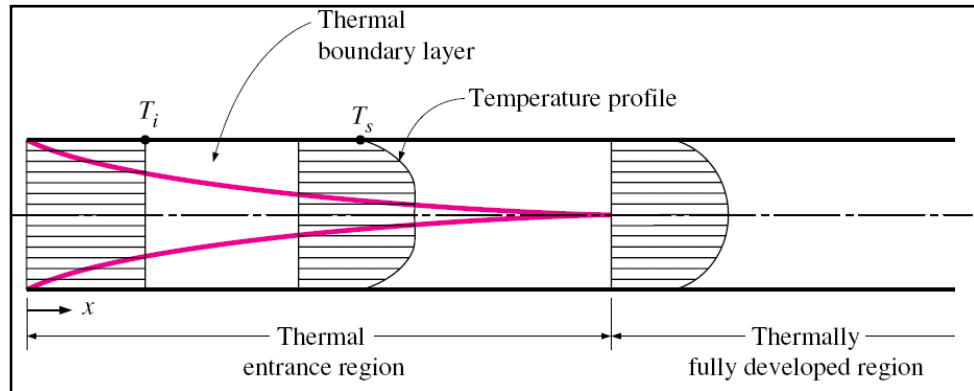
Figure 2.3: Developing Thermal Boundary Layer in Tube

Source: Cengel (2006)

For turbulent flow, the entry length can be determined from Bhatti and Shah, (1987) and Zhi-qing, (1982) as follow.

$$L_{h,turbulent} = 1.359D \, Re^{1/4} \tag{2.5}$$

$$L_{h,turbulent} \approx L_{t,turbulent} \approx 10D \tag{2.6}$$

2.5.6   Laminar And Turbulent Flow In Tubes

Flow in a tube with low velocities is call laminar flow. Laminar flow is encountered when highly viscous fluids such as oils flow in small diameter tubes or narrow passages. Flow becomes laminar when the Reynolds number, Re < 2300.

However, most of the pipe flows encountered in practice are turbulent. The main reasons of utilizing turbulent flow because of higher heat transfer coefficients associated

with it. Most of correlations for friction and heat transfer coefficient for turbulent flow are obtained based of experimental studies because of very difficult in dealing with turbulent flow in theoretically. Normally, flow becomes fully turbulent for $Re > 10,000$ but in some cases the turbulent flow occurs for $Re > 4000$. In designing piping network and pumping power, a conservative approach is taken and flow with $Re > 4000$ is considered as turbulent flows.

2.5.7 Constant Surface Heat Flux ($\dot{q}_s$ = constant)

The thermal conditions at the surface can usually be approximated with reasonable accuracy either constant surface temperature (T_s = constant) or constant surface heat flux ($\dot{q}_s$ = constant). In the case of constant surface heat flux, the tubes are subjected to the radiation or electric resistance heating uniformly from all direction. The rate of heat transfer in this case can be express in Eq. 2.7.

$$\dot{Q} = \dot{q}_s A_s = \dot{m} C_p (T_e - T_i) \qquad \text{(W)} \tag{2.7}$$

Where, T_e is the temperature exit and T_i is the temperature inlet. However, the mean fluid temperature at the tube exits shown in Eq. 2.8.

$$T_e = T_i + \frac{\dot{q}_s A_s}{\dot{m} C_p} \tag{2.8}$$

The surface temperature in the case of constant heat flux can be determined from Eq. 2.9

$$\dot{q}_s = h(T_s - T_m) \rightarrow T_s = T_m + \frac{\dot{q}_s}{h} \tag{2.9}$$

In the fully developed region, both $\dot{q}_s$ and h are constant and the surface temperature T_s will also increase linearly in the flow direction as shown in Figure 2.4.
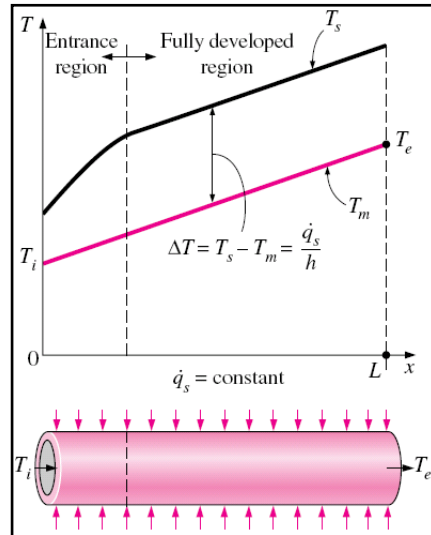
Figure 2.4: Variation of the tube surface and the mean fluid temperature under constant heat flux conditions

Source: Cengel (2006)

2.5.8 Constant Surface Temperature (T_s = Constant)

In conditions of constant surface temperature, condition is realized when phase change process such as boiling or condensation occurs at outer surface of a tube. The rate of heat transfer to or from fluid flowing in tube can be express by Newton's law of cooling in Eq. 2.1.

The term of h, A_s, T_s and T_m are same with the previous discussion but for the term ΔT_{avg}, it can be expressed approximately by the arithmetic mean temperature difference, ΔT_{am} in conditions of constant surface temperature as shown in Eq. 2.10.

$$\Delta T_{avg} \approx \Delta T_{am} = \frac{(T_s - T_i) + (T_s - T_e)}{2} \qquad (2.10)$$

Arithmetic mean temperature difference ΔT_{am} is simply the average of the temperature differences. This simple approximation often gives acceptable results but

not accurate. Figure 2.5 shown the temperature difference are decrease when through a constant surface temperature tube and always below the surface temperature at tube exit.
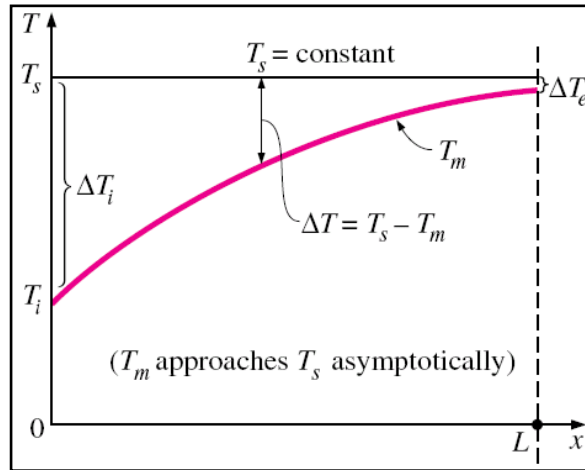
Figure 2.5: Variation of the mean fluid temperature along the tube for the case of constant temperature

Source: Cengel (2006)

Therefore, logarithmic mean temperature difference is introduced to approximate the best result for constant surface temperature conditions with modify Newton's law of cooling in Eq. 2.11.

$$\dot{Q} = mC_p = hA_s\Delta T_{lm} \tag{2.11}$$

Where, ΔT_{lm} is express in Eq. 2.12.

$$\Delta T_{lm} = \frac{T_i - T_e}{ln\left[(T_s - T_e)/(T_s - T_i)\right]} = \frac{\Delta T_e - \Delta T_i}{ln\left[\Delta T_e/\Delta T_i\right]} \tag{2.12}$$

Note that, for condition at a constant surface temperature, logarithmic mean temperature difference is preferred when determining the convection heat transfer in a tube.

2.5.9 Pressure Drop

Pressure drop is one of the interests in analysis since it is directly related to the power requirement of the fan or pump to maintain the flow. In fluid flow, pressure drop is designated as ΔP and its represent the difference between final and initial of pressure. Then, due to viscous effect represent irreversible pressure loss, pressure drop is called pressure losses indicated by ΔP_L to emphasize that it is a loss.

In practice, convenient equation is found to express the pressure loss for fully develop internal flows (laminar and turbulent flows, circular or noncircular pipes, smooth or rough surfaces, horizontal or inclined pipes) as shown in Eq. 2.13

$$\Delta P_L = f \frac{L}{D} \frac{V_{avg}^2}{2} \qquad (2.13)$$

Where, f is the Darcy friction factor or Darcy-Weisbach friction factor. Solving for f gives the friction factor for fully developed laminar flow in a circular tube using Equation 2.14.

$$f = \frac{64\mu}{\rho D V_{avg}} = \frac{64}{Re} \qquad (2.14)$$

Since Eq. 2.14 is only valid for fully developed laminar flow, another equation is used to determine the friction factor turbulent flow known as the Colebrook equation shown in Eq. 2.15.

$$\frac{1}{\sqrt{f}} = -2.0 \log\left(\frac{\varepsilon/D}{3.7} + \frac{2.51}{Re\sqrt{f}}\right) \qquad (2.15)$$

Where, ε is relative roughness of the material and different value with different material. Lewis F. Moody (1880-1953) verified Colebrook equation and represent as a graphical plot known as Moody chart as given in Appendix A. It is present Darcy

friction factor for pipe flow as a function of the Reynolds number and ε/*D* over a wide range also one of the accepted and used charts in engineering.

Once the pressure loss is known, the required pumping power to overcome the pressure loss is determine from Eq. 2.16

$$\dot{W}_{pump,\,L} = \dot{V}\Delta P_L = \dot{V}\rho g h_L = \dot{m} g h_L \qquad (2.16)$$

Where, $\dot{V}$ is the volume flow rate can be calculate by using basic equation $\dot{V} = V_{avg}A_c$ and A_c is the cross sectional area of the pipe or tube. While, $\dot{m}$ is the mass flow rate and can be calculate by using $\dot{m} = \rho V_{avg}A_c$.

2.6 ENGINEERING PARAMETER

Common practice in engineering studies to nondimensionalize the governing equations and combines the variables, which group together into dimensionless number in order to reduce the number of total variables. It also to standardize the result obtains from various experimental with different parameter used. Thus, dimensionless is the best method to make a comparison between other researchers' results.

2.6.1 Heat Transfer Coefficient (HTC)

Heat transfer performance is a better indicator than the effective thermal conductivity for nanofluid used in industry. Heat transfer coefficient is indicated by *h* and the value is depends on the type of the fluid gas or liquid, the properties of the flow and temperature of the flow. The value of HTC can be obtained by applying the Nusselt number equation as shown in Equation 2.17, 2.18, 2.19, 2.21, and 2.22 with respect to the properties of the flow either fully developed laminar or turbulent flow and surface roughness of the tube wall.

Normally, the internal pipe flow convection coefficient of nanofluids was measured experimentally. Nanofluid was dilute to various volume fractions and particles size for convection heat transfer coefficient study. The high volume fraction

results in the high viscosity of the fluid and a tendency for the nanoparticles to stick on the walls of tubing and containers. It also requires large pumping power. Therefore, the highest concentration of the testing fluid is limited since higher cost for nanoparticles.

2.6.2 Nusselt Number (*Nu*)

The Nusselt number is named after Wilhelm Nusselt, who make significant contributions to convective heat transfer in the first half of the twentieth century and it's viewed as the dimensionless convection heat transfer coefficient. Nusselt number also defined as the ratio of heat transfer by convection and conduction across the same fluid. The larger the Nusselt number, the more effective the convection. In convection studies, it common practices to nondimensionalize the heat transfer coefficient, with the Nusselt number defined as Eq. 2.17

$$Nu = \frac{hD}{k} \tag{2.17}$$

Where k is the thermal conductivity of the fluid, h is heat transfer coefficient of the fluid and D is the diameter of the tube.

Another alternative to obtain Nusselt number is given by Gnielinski Equation (Gnielinski, 1976) as given in Eq. 2.18 and valid in the range of $2300 < Re < 5 \times 10^6$ and $0.5 < Pr < 2000$.

$$Nu = \frac{\left(\frac{f}{2}\right)(Re\text{-}1000)Pr}{1 + 12.7\left(\frac{f}{2}\right)^{0.5}\left(Pr^{\frac{2}{3}}\text{-}1\right)} \tag{2.18}$$

Where friction factor, f can be determined from the first Petukhov equation as given in Eq. 2.19,

$$f = (1.58 \ln Re - 3.82)^{-2} \tag{2.19}$$

For fully developed turbulent flow in smooth tubes, Dittus-Boelter equation (Dittus and Boelter, 1930) shown in Eq. 2.20 is obtained to improve the accuracy from the Colburn equation.

$$\text{Nu}=0.023\,Re^{0.8}Pr^{n}=\begin{cases} Re>10{,}000, & n=0.4 \text{ heating} \\ 0.7 \leq Pr \leq 160, & n=0.3 \text{ cooling} \end{cases} \qquad (2.20)$$

Sharma et al., (2009) has developed a regression equation which valid for both water and nanofluid flow through plain ube and twisted tape having volume concentration less than 0.1% and given by Eq. 2.21.

$$Nu_{Reg}= 3.138\times10^{-3}(Re)(Pr)^{0.6}\left(1.0+\frac{H}{D}\right)^{0.03}(1+\varphi)^{1.22} \qquad (2.21)$$

Equation 2.21 is valid for water ($\varphi = 0$) and for flow in plain tube (H/D) = 0

Sarma et al., (2010) has developed new equation to predict Nusselt number for nanofluids with different concentration and as shown in Eq. 2.22.

$$Nu = 0.0304\, Re^{0.7853}Pr^{0.4}(0.01+\emptyset)^{0.01398} \qquad (2.22)$$

Where $\emptyset$ is concentration of nanofluids and can be replace by 0 for pure water.

2.6.3   Reynolds Number (*Re*)

Osborn Reynolds discovered in 1880s that the flow regime depends mainly on the ratio of the inertia forces to viscous forces as shown in Equation 2.23. This ratio is called the Reynolds number which is dimensionless quantity.

$$Re = \frac{Inertia\ Forces}{Viscous\ Forces} = \frac{V_{avg}D}{v} = \frac{\rho V_{avg}D}{\mu} \qquad (2.23)$$

Where D is diameter of the tubes, ρ is density of the fluid, v is kinematic viscosity, and μ is dynamic viscosity of the fluid.

From the derivation of Eq. 2.23, Reynolds number also can express as shown in Eq. 2.24.

$$Re = \frac{4\dot{m}}{\pi D_i \mu}$$ (2.24)

2.6.4 Prandtl Number (*Pr*)

Prandtl number is described of the relative thickness of the velocity and the thermal boundary layers. It is name after Ludwig Prandtl, who introduced the concept of boundary layer in 1904 and make significant contribution to boundary layer theory. The prandtl numbers of fluid range from less than 0.01 for liquid metals to more than 100,000 for heavy oils. The Prandtl number is defined as in Eq. 2.25.

$$Pr = \frac{Molekular\ diffusivity\ of\ momentum}{Molekular\ diffusivity\ of\ heat} = \frac{v}{\alpha} = \frac{\mu C_p}{k}$$ (2.25)

The Prandtl number of gases is about 1, which indicates that both momentum and heat dissipate through the fluid at the same rate. Heats diffuse very quickly in liquid metals (*Pr* < 1) and very slowly in oils (*Pr* > 1). Consequently the thermal boundary layer is much thicker for liquid metals and much thinner for oils relatively to the velocity boundary layer.

2.7 PREVIOUS EXPERIMENTAL INVESTIGATION

Nanoparticles made from metal oxides, metals, nanotubes and graphite are widely investigated in based fluids such as water, ethylene glycol, and acetone. There are researches carry out by previous researcher with related to this study.

2.7.1 Experiment with Metal Oxide Nanoparticles

Eastman, et. al. (1999) is conducted test to access the thermal performance of CuO/water with volume concentration, $\emptyset = 0.9\%$ under turbulent flow conditions and

found the heat transfer coefficient was higher by 15% than that pure water. Pak and Cho, (1998) has presented an experimental investigation of the convective turbulent heat transfer characteristic of nanofluids Al_2O_3-water and TiO_2-water with volume concentration, $\emptyset$ between 1 to 3% and found the Nusselt number for the nanofluids increased with an increasing volume concentration and Reynold number. Williams et. al. (2008) has investigated the turbulent convective heat transfer behavior of Al_2O_3/water and ZrO_2/water. The result found the convective heat transfer and pressure loss behavior of nanofluids under fully developed turbulent flow is matched the correlations of a single phase flow. Jang and Choi, (2004) showed an enhancement of the convective heat transfer coefficient of nanofluids (Al_2O_3/water with $\emptyset = 0.3\%$) up to 8% from their based fluid. Duangthongsuk and Wongwises, (2009) reported an experimental study on the forced convective heat transfer under varied heat flux boundary conditions and pressure drop characteristics of a nanofluid consisting of water and 0.2% TiO_2 nanoparticles of 21nm diameter flowing in a horizontal double tube counter flow heat exchanger under turbulent flow conditions found the results slightly higher than the base fluid about 6 to 11%. The heat transfer coefficient of the nanfluid is increases with increase in the mass flow rate of the hot water and nanofluid. Torii, (2009) has performed experimental study to investigate heat transfer performance of adequos suspension of nanoparticle Al_2O_3, CuO and diamond and found that the relative viscosity of nanofluids increase with an increase of volume concentration of nanoparticles, and the increase rate of the viscosity for nanofluid is different by particles. Therefore, the pressure loss of the nanofluids tends to increase slightly compared to pure water and heat transfer performance in the circular tube flow is amplified by suspension of nanoparticles. Fotukian & Esfahany, (2009) claimed that the Al_2O_3/water nanofluid convective heat transfer in turbulent regime inside a circular tube with nanoparticles volume fractions less than 0.2% have heat transfer coefficient increased about 48% compared to pure water. Increasing the nanoparticles concentration does not show much effect on heat transfer enhancement in turbulent regime in the range of concentrations studied. Also the ratio of convective heat transfer coefficient of nanofluid to that of pure water decreased with increasing Reynolds number. It is observed that the wall temperature of the test tube decreased considerably when the nanofluid flowed in the tube. The maximum increase in pressure drop was about 30% for nanofluid with 0.135% volume concentration at Reynolds number of 20,000.

2.7.2 Experiments with Pure Metal Nanoparticles

Xuan and Li, (2003) studied the single phase heat transfer of the Cu/water nanofluid in tubes in the turbulent regime (10,000 < Re < 25,000) with $\emptyset$ = 0.3 to 2.0%. The results found that the convective heat transfer coefficient increased remarkably with the volume fraction and with the flow velocity, with negligible penalty in pumping power. Zhou, (2004) has investigated the enhancement of the single phase heat transfer of Cu-acetone particles with average particles size in the 80-100nm range and concentrations between 0.0 to 4.0 g/l. The result found the convective heat transfer coefficient increases with addition of Cu nanoparticles. Xuan, et al., (2005) investigated Cu/water (deionised) with 26nm size of nanoparticles and volume concentration between 0.5 and 2.0%. The result found the Nusselt number increased proportionately with the Reynolds number and the Nusselt number ratio between Cu/water varied from 1.06 to 1.39 when the volume fraction of copper nanoparticles increased from 0.5 to 2.0%.

2.7.3 Experimental study on Convective Heat Transfer

Experimental study by Shen, (2008) are using Al_2O_3 nanofluid with various volume fraction with water as a base fluid was carry out and the result as shown in Figure 2.6. All the Al_2O_3 nanofluids have higher Nusselt number than water under the same Reynolds number. Generally, the Nusselt number increases with increasing Reynolds number as well as the volume fraction of the suspended Al_2O_3 nanoparticles.

However, the experimental results shown in Figure 2.7, there is no significant difference between the Al_2O_3 nanofluids and based fluid when interpreting in term of flow rate and convection heat transfer coefficient. This is mainly due to higher viscosity of nanofluid. The nanofluids with higher viscosity have the higher Nusselt number under the same Reynolds number, which is actually corresponding to a higher flow rate.
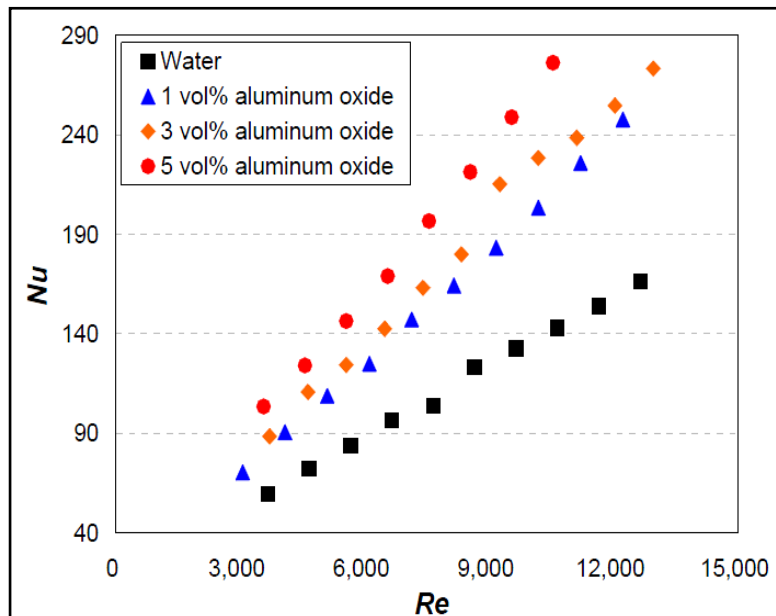
Figure 2.6: Nusselt number Versus Reynolds number

Source: Shen (2008)
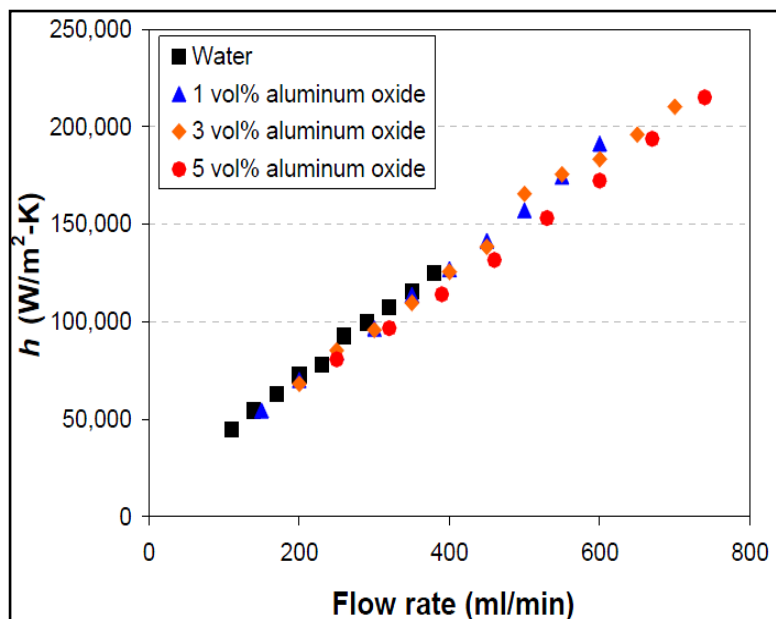
Figure 2.7: Hear Transfer Coefficient versus Flow rate

Source: Shen (2008)

2.7.4   Conclusion on Previous Experimental Studies Results

The observed results from the prior work done on the convective heat transfer performance of nanofluids clearly shows, that the suspended particles outstandingly increase the heat transfer performance of the base-fluid and the nanofluids have higher heat transfer coefficients and thermal conductivity than those of the base-fluids at the same Reynolds number. High aspect ratio nanoparticles such as carbon nanotubes resulted in greater enhancement in thermal conductivity and the heat transfer coefficient. It has been shown in many references that the heat transfer behavior of nanofluids and the application of nanofluids for heat transfer enhancement, are influenced by the effective thermo-physical properties of nanofluids and many other factors such as particle size, shape and distribution, Brownian motion, particle fluid interaction and particle migration also have an important influence on the heat transfer performance of nanofluids. The summaries of experimental investigations that are related with this study in convective heat transfer of nanofluids are shown in Table 2.4.

Table 2.4: Summary of Experimental Investigations in Convective Heat Transfer of Nanofluids with Water Based Fluid

Author	Particle Material	Particle Size	Volume Fraction (Vol. %)	Dimension	Flow Regime	Result and Remark
Pak and Cho.	Al_2O_3	13nm	1-3	ID: 1.066cm	Re = 10^4-10	Nu increased with
	TiO_2	27nm	1-3	Length:	(Turbulent	increase in $\emptyset$ and
				480cm	Flow)	Re.
				S/S tube		
Eastman et al.	CuO	< 100nm	0.9	-	Turbulent Flow	HTC increased by >15% compared with pure water
Williams et al.	ZrO_2	46nm	0.9-3.6	OD:1.27cm	9000 < Re <	Matched the
	Al_2O_3	60nm	0.2-0.9	Thick =	63,000	correlation of single
				1.65mm	(Turbulent	phase flow
				S/S tube	flow)	

Table 2.4: Continued

Author	Particle Material	Particle Size	Volume Fraction (Vol. %)	Dimension	Flow Regime	Result and Remark
Duangthongsuk and Wongwises	TiO2	21nm	0.2	Horizontal double tube counter flow heat exchanger	(Turbulent flow)	HTC increased 6-11% compared with base fluid
Jang and Choi	Al2O3	-	0.3	-	-	HTC increased up to 8%
Xuan and Li	Cu	<100nm	0.3 – 2.0	ID: 10mm Length: 800mm Brass tube	10,000 < Re < 25,000 (turbulent flow)	HTC increased with increasing ∅ and flow velocity
Xuan et al.	Cu	26nm	0.5 - 2.0	ID: 10mm Length: 800mm Brass tube	1000 < Re < 4000	Nu ratio varied from 1.06 to 1.39 when ∅ increases from 0.5% - 2%

Source: Godson et al. (2010)

2.8   PREVIOUS MATHEMATICAL INVESTIGATION

The mixture of nanoparticles with base fluid is a multiphase fluid and it could be approximated as either a homogeneous fluid or heterogeneous mixture. Homogeneous fluid is considered single phase fluid since it may easily be fluidized and by assuming a negligible motion slip between the particles and the thermal equilibrium conditions, the nanofluid could be considered as a conventional single phase fluid with average physical properties of individual phase (Pak and Cho, 1998). Heterogeneous (two-phase) is consider factors such as gravity, friction between the phases, Brownian diffusion, sedimentation and dispersion into their model.

2.8.1 Theoretical Investigations

Buongiorno, (2006) have developed an alternative model that eliminates the shortcomings of the homogeneous and dispersion models. Detailed analysis of convective transport is divided into seven slip conditions between particles and fluid for explaining the enhancement of heat transfer with nanofluids. Convective heat transfer enhancement was obtained with a decrease in viscosity and consequent thinning of the laminar sub layer. It was observed that the radial distribution of the particle concentration is more concentrate at the core than walls brought about by thermophoresis make the temperature profile flatten and higher heat transfer coefficient.

Maiga et al., (2003) modeled the forced convection flow of nanofluid (Al_2O_3) with water and ethylene glycol in a straight tube of circular cross section. A single phase flow is assumed to derive governing equations. With nanofluid concentrations ranging from 0 to 10%, the results found an increase in heat transfer coefficient ratio by nearly 60%. For turbulent flow region, heat transfer coefficient is increased steeply for a very short distance from the inlet section.

Mansour et al., (2007) have investigated the effect of the Hamilton Crosser model and the Modified Maxwell model, to predict nanofluid (Al_2O_3/water; $\emptyset = 1$ to 10%) physical properties, on their thermal and hydrodynamic performance for both fully developed laminar and turbulent forced convection in a tube with uniform heat flux at the wall. Two models gave substantially different results for thermal conductivity, specific heat and viscosity, and the differences were more profound for higher particle loading. The expressions failed to account for the size disparity between the nanoparticles. The study illustrated that the operational conditions or the design parameters varied significantly with the thermo-physical properties of the nanofluid. However, both models are predicted of increase of heat transfer coefficient when particle concentrations increase.

2.8.2 Conclusions from Theoretical Studies with Nanofluids

The observations based on the reviewed literature for theoretical studies in the convective heat transfer of nanofluids clearly shows, that the models developed by the various researchers have been satisfactory only under very stringent conditions. However, a generalized theoretical model should be developed by considering all the factors such as inertia, thermophoresis, Brownion motion, and gravity which influences the heat transfer characteristics and the behavior of nanofluids under convective heat transfer conditions. The summary of the theoretical investigations in the convective heat transfer of nanofluids is given in Table 2.5.

Table 2.5: Summary of Theoretical Investigations in Convective Heat Transfer of Nanofluids.

Author	Theoretical investigations	Approach	Results and Remarks
Buongiormo	Convective transport in nanofluids	Two-component nonhomogeneous equilibrium model	Brownian diffusion and thermophoresis are the two most important for nanoparticles/basefluid slip mechanism
Behzadmehr et al.	Turbulent forced convection flow in a uniformly heated tube	Two-phase mixture model	HTC increases with $\emptyset$ and Re. Higher Re resulted more uniform velocity profile
Maiga et al.	Forced Convection flow of nanofluid (water/Al_2O_3 and ethylene glycol/ Al_2O_3) in a circular tube	Single phase fluid approach	60% enhancement in HTC was found and turbulent flow enhancement increases with Re
Mansour et al.	Thermal and hydrodynamic performance for both laminar and turbulent forced convection in a tube with uniform heat flux at the wall	Single phase fluid approach	Both the model predicted increased HTC with particle concentration

Source: Godson et al. (2010)

2.9 THERMOPHYSICAL PROPERTIES

Thermophysical properties of material or fluids are very important value in analysis since it affecting the transfer and storage of the heat that vary with the state variables temperature, pressure and composition without altering the materials and chemical identity. There are two ways to determine the thermophysical properties of nanofluids which are from experimental using appropriate apparatus and correlation develop from previous researchers. Measurement apparatus used in determine thermophysical properties such as thermal conductivity, density, specific heat and viscosity will be explained on the next subchapter.

2.9.1 Thermal Conductivity

Transient hot-wire apparatus is used to measure thermal conductivity of fluid. It can accurately measure in the liquid, vapor and supercritical fluid phases of pure fluids and mixtures at temperatures from 30 K to 750 K with pressures to 70 MPa. One of the hot-wire apparatus is shown in Figure 2.8, and it used 4 micron diameter tungsten, 12.7 micron diameter platinum, or 25 micron diameter anodized tantalum (electrically insulated) hot wires depending on the fluid of interest. Electrically conducting fluids require the use of insulated hot wires.

In the transient hot-wire technique, small diameter wires are immersed in the fluid and used simultaneously as electrical resistance heaters and as resistance thermometers to measure the resulting temperature rise due to the resistance heating. The hot-wire cells are designed to approximate a simple 1-dimensional transient line-source of heat in an infinite medium as closely as possible to minimize corrections for the actual geometry. Two hot wires of differing length are operated in a differential mode to eliminate axial conduction effects due to the large diameter leads attached to the ends of each hot wire. Based on the transient line-source model, the thermal conductivity can be found from the slope of the measured linear temperature rise as a function of elapsed time with a typical uncertainty of less than 1%.
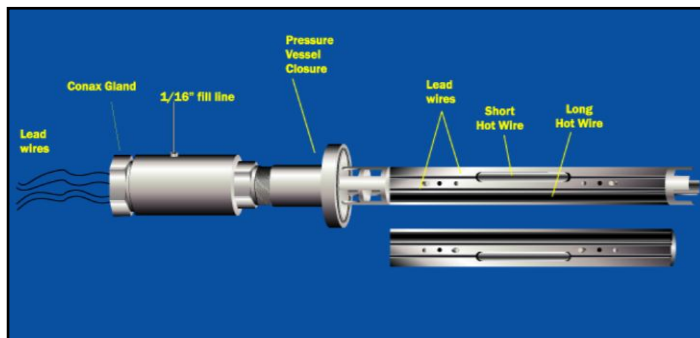
Figure 2.8: Hot-Wire Apparatus

Source: National Institute of Standard and Technology (2010)

2.9.2   Density

There are various possible methods in determining the density of unknown fluids such as isochoric method, variable volume method, the Burnett method, Buoyancy force device, vibrating tube densimeter, pulse method and etc. It is possible to estimate the density of a liquid using a pulse method which utilizes pulse-echo ultrasound to estimate density of unknown fluid. The setup consists of an ultrasonic piezoceramic disk which is separated from the liquid sample by a buffer rod with known properties. A reflector within the liquid perpendicular to the sound path reflects the pulse to estimate the speed of sound in the liquid as shown in Figure 2.9.
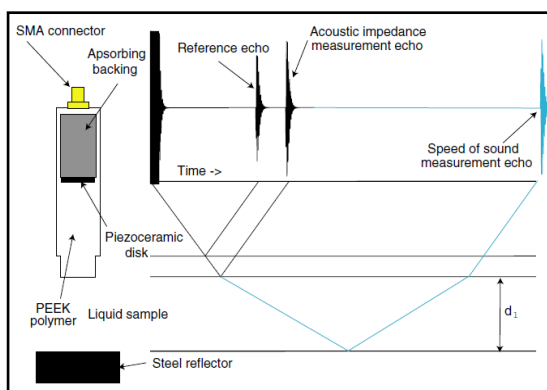
Figure 2.9: The Lynn worth densitomer with its associated lattice diagram

Source: Deventer (2004)

2.9.3 Specific Heat

Usually specific heat is measured by calorimeter. Many kinds of calorimeters have been constructed such as isothermal calorimeter, heat flux calorimeter, adiabatic calorimeter, flow calorimeter and etc. It is quite impossible to give a complete description of the devices that have been presented in the literature or are commercially available. All the efforts have consisted of attempts to approach ideal calorimeters or to improve the methods for accurate control and estimation of the corrections.

In analysis of specific heat on fluid, flow calorimeter is used which fluid samples flowing through the flow calorimeter as shown in Figure 2.10. A known amount of heat per unit time is injected in a constant fluid flow entering the calorimeter at the initial temperature, T_i. The specific heat (more precisely, the enthalpy change) is calculated from Eq. 2.10 which is from the input power W, the temperature difference of the fluid between final temperature, T_f and inlet temperature, T_i and the fluid flow, $\dot{m}$.
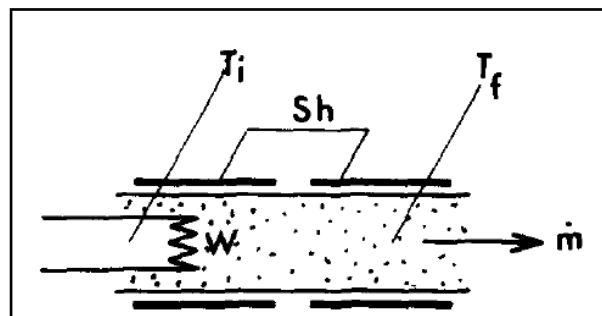
Figure 2.10: Flow Calorimeter

Source: Tufeu (1989)

2.9.4 Viscosity

Viscosity is a principal parameter when any flow measurements of fluids, such as liquids, semi-solids, gases and even solids are made. There are many different techniques for measuring viscosity, each suitable to specific circumstances and materials. Some employ capillary flow method, rising bubbles, falling or rolling balls,

vibrating wire and etc. However, commonly viscometer used is rotational (Brookfield) type which is measures the force required to rotate a disc or hollow cup immersed in the specimen fluid at a predetermined speed. As the disk or hollow cup is rotated, the viscous drag of the fluid against the disk or hollow cup is measured by the deflection of the calibrated spring. Figure 2.11 is show the example of Rotational viscometer (Brookfield type).

(a)   (b)
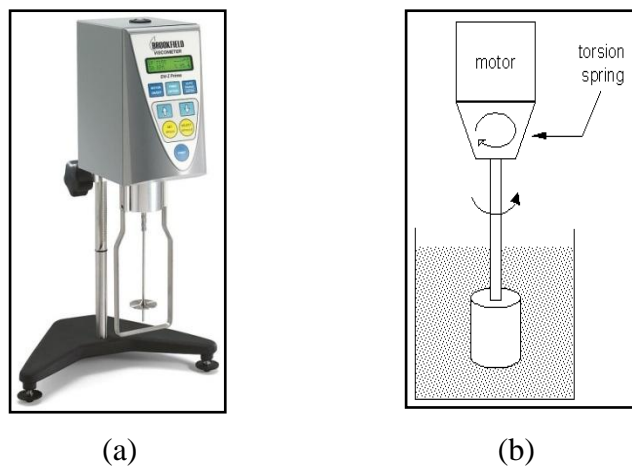
Figure 2.11: Rotational Viscometer (Brookfield type)

Source: Brookfield engineering (2010)

2.9.5   Thermo-physical Properties Correlation

Popular correlation to predict thermo-physical properties of nanofluids have shown below:

Pak and Cho, (1998) Eq.

$$\mu_{nf} = \mu_w(1 + 39.11\emptyset + 533.9\emptyset^2) \tag{2.26}$$

$$k_{nf} = k_w(1 + 7.47\emptyset) \tag{2.27}$$

$$\rho_{nf} = \emptyset\rho_p + (1\text{-}\emptyset)\rho_w \tag{2.28}$$

$$C_{nf} = C_p + (1-\emptyset)C_w \tag{2.29}$$

Azmi, et al. (2010) has introduced regression equation to predict thermophysical properties of water based on bulk temperature as shown in Eq. 2.26 to Eq. 2.29.

$$\rho_w = 1000 \times \left[1.0 - \frac{(T_b - 4.0)^2}{119000 + 1365 \times T_b - 4 \times (T_b)^2} \right] \tag{2.26}$$

$$\mu_w = 0.00169 - 4.2563e^{-5} \times T_b + 4.9255e^{-7} \times (T_b)^2 - 2.0993504e^{-9} \times (T_b)^3 \tag{2.27}$$

$$k_w = 0.56112 + 0.00193 \times T_b - 2.60152749e^{-6} \times (T_b)^2 - 6.08803e^{-8} \times (T_b)^3 \tag{2.28}$$

$$C_{p_w} = 4217.629 - 3.20888 \times T_b + 0.09503 \times (T_b)^2 - 0.0132 \times (T_b)^3 + 9.415e^{-6}$$
$$\times (T_b)^4 - 2.5479e^{-8} \times (T_b)^5 \tag{2.29}$$

2.10 ADVANTAGES AND DISADVANTAGES OF NANOFLUIDS

Nanofluids is found to have a great advantages in heat transport, it is approved by previous researchers during evaluate their thermal performance. However, it also has disadvantages discovered in nanofluids. Advantages and disadvantages of nanofluids are explained in the next subchapter.

2.10.1 Advantages

Nanofluids have great advantages which can be followed from the properties of metallic or non-metallic particles that are added to base fluids. Most of nanofluids have been studied about experiments of thermal conductivity and mechanism of heat transfer enhancement and reported that heat transfer performance and their thermal conductivity is increased compared to common fluids. In application of cooling system, it can reduce the size, weight and cost of thermal apparatus. For example, application of nanofluids in

engine cooling system that remove engine heat with reduced size coolant system resulted in smaller and lighter radiators, which in turn benefit almost every aspect of vehicle performance and lead to increased fuel economy.

Numerous advantages of nanofluids such as no clogging, no stationary bed in a flow through a tube and low pressure drop when particles sizes close to nanoscale or even nanosize have found by previous researchers.

2.10.2 Disadvantages

Some of the researchers claimed that there is no erosion when nanofluid flowing through a tube but in case of improper in the process of nanofluid preparation resulted of agglomeration. When it's occurs, it is important to consider surface erosion caused by the flowing fluid as well as effects of particle settling and agglomeration. The effects of agglomeration and settling need serious attention. The dispersion and suspension of nanoparticles in a fluid pose a difficult colloidal chemistry problem, and considerable work remains to be done if the two-step process is ever to develop into large scale production.

Other disadvantages of nanofluids is the challenge in producing process of nanoparticles since the existing process consume higher cost, thus it is limited to produce nanofluid in a large scale.

2.11   CONCLUSION

Nanofluids have a bright future to be used as an effective heat transfer fluids and have greater potential for heat transfer enhancement and are highly suited to application in practical heat transfer processes. This is an opportunity for engineers to develop highly compact and effective heat transfer equipment. Several published articles show that the heat transfer coefficient of nanofluids is much higher than that of the common-base fluid and gives little or no penalty in pressure drop. Therefore, further research on convective heat transfer of nanofluids and more theoretical and experimental research works are needed in order to clearly understand and accurately predict the trend for heat transfer enhancement.

CHAPTER 3

RESEARCH METHODOLOGY

3.1   INTRODUCTION

This chapter describes in details how this study will progress from the calibration of apparatus until it complete. In this research, the main concern is determination of convective heat transfer coefficient of nanofluids which is estimate from experimental study to generated base data by measuring the heat transfer on the test section. By using this data, convenience graph and dimensionless result is obtained to validate with previous research result and numerical study result. Method of experimental setup, parameters and analysis of data gather from an experiment is explained in this chapter.

Finally, overall process and step by step how to carry on this research from the beginning until the end was shown in Figure 3.1 in order to successfully complete this project.

3.2   RESEARCH FLOWCHART

The flowchart of this research is separate into three phase which is pre-experiment, experiment and post-experiment. It is shown in Figure 3.1. In pre-experiment, experiment is set up and calibrates the apparatus then sample of nanofluids is prepared and proceed to thermophysical properties. While during experiment, it is run a various range of Reynolds number and data were collected. At the post experiment stage, analysis was carried out and verified with previous researchers result and numerical study results.
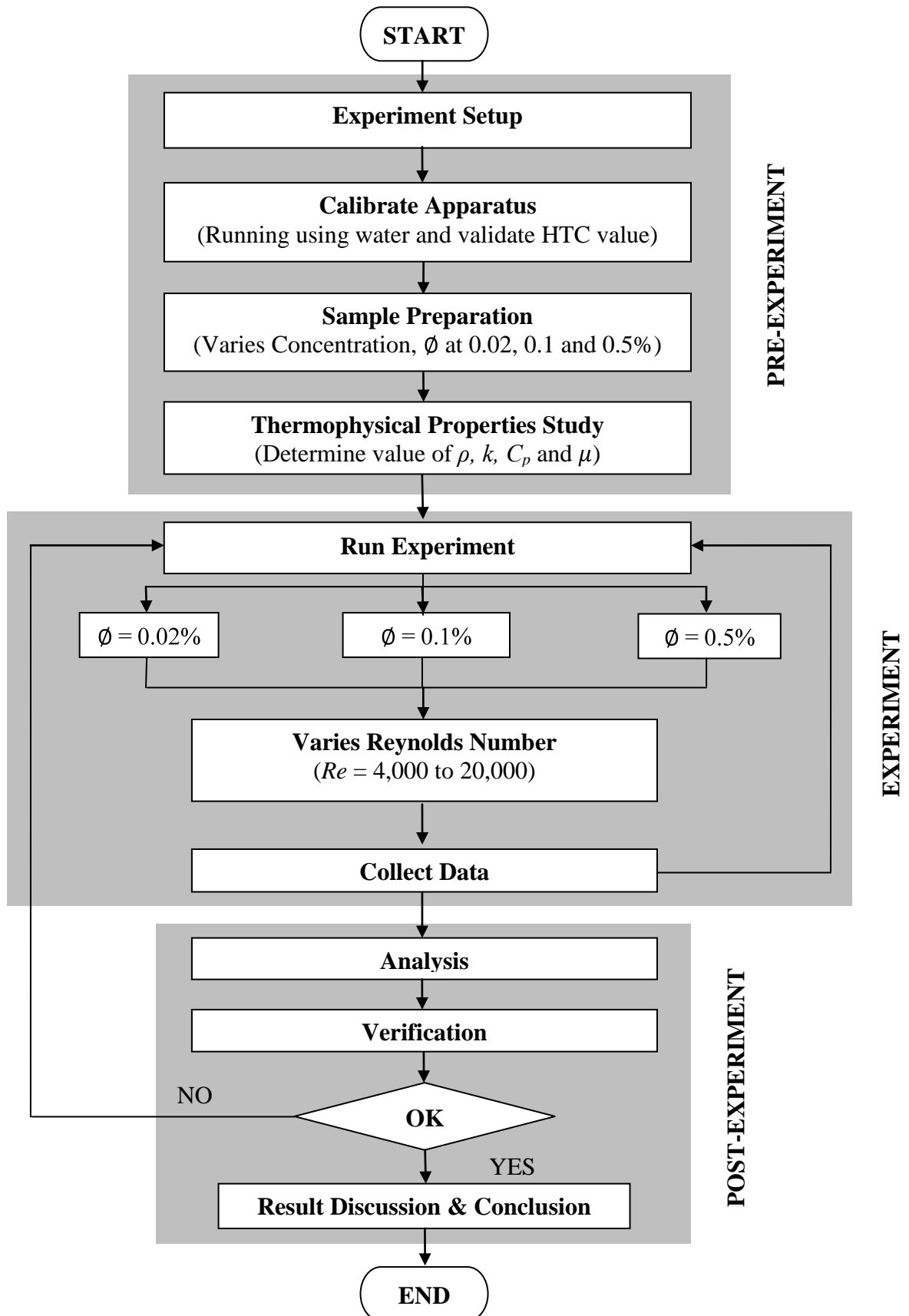
Figure 3.1: Research Flowchart

3.3 EXPERIMENTAL SET UP

The schematic diagram of the experimental set up is shown in the Figure 3.2. The set up consist of apparatus such as circulating pump, totalizer, heater, control panel, thermocouples, chiller, receiving tank, collecting tank and test section consist of copper tube with diameter of 0.019 m length 1.5 m. However, the total length of tube in this experiment is 3.0 m length.

The working fluid (sample fluid) is circulated through the loop by using variable speed to achieve different parameters in this study. The working fluid is stored in the collecting tank made by stainless steels with 30 liter capacity after sample preparing. From Eq. 2.6, the length of hydronamically thermal entrance region was calculated to be 0.19 m which is much less than the total length and ensures the flow to be fully hydronamically and thermally developed.

The tube is heated uniformly for a 1.5 m length test section by wrapping with two nichrome heater 20 gauge with 570W electric rating. The tube was insulated by rock wool insulation to minimize heat loss to atmosphere. Five thermocouples are located on varies distances which is three at the surface of the tube wall with 0.375, 0.75, 1.125 m from the inlet and the other two are measure inlet and outlet temperature of the test section.

3.4 CALIBRATION APPARATUS

The accuracy and reliability of the experimental apparatus system were tested before measuring the convective heat transfer coefficient. This was carried out by using water as the working fluid and the result obtained of the convective heat transfer coefficient were compared with the predicted values obtained from Gnielinski Equation as define in Eq. 2.18 under sub-topic 2.6.2.

3.5   SAMPLE PREPARATION

The term 'nanofluid', meaning a two-phase mixture usually consists of nanoparticles dispersed in common liquids. There are two techniques to produce a nanofluid which is single step and two step techniques but most of nanofluids containing oxide nanoparticles and carbon nanotube is produce by the two step techniques.

In this experiment, nanofluids are prepared by two step techniques which dispersing the nanoparticles in a base fluid in this study is water, proper mixing, and stabilization of the particles. There are three methods used to attain stability of suspension against sedimentation of nanoparticles, and these are summarized as follows:

    i.   Control of ph value of the suspensions.

    ii.   Addition of surface activators or surfactants (Sodium Dodecyl Benzene Sulfonate - SDBS).

   iii.   Use of magnetic stirrer for continuously mixture.

Al_2O_3 nanoparticles with average diameter size of 50 nm are supplied by Sigma-Aldrich Chemicals Ltd., Germany and distilled water is used to prepare the nanofluid. Sodium Dodecyl Benzene Sulfonate (SDBS) is weighing 10% from the mass of nanoparticles and used as dispersant to stabilize the nanoparticles in the base fluid. Nanoparticles are added after the dispersant is mixed with water around tenth minutes. The mixture is stirred with magnetic stirrer continuously for 10 hours. The desired volume concentrations used in this study are 0.02%, 0.05%, and 0.5%, with pH values of 7.1, 7.0, and 6.8, respectively. From the pH values, it can be seen that the solution chemistry of nanofluids is nearly neutral in nature. Figure of nanofluids preparation have been illustrated in Appendix F.
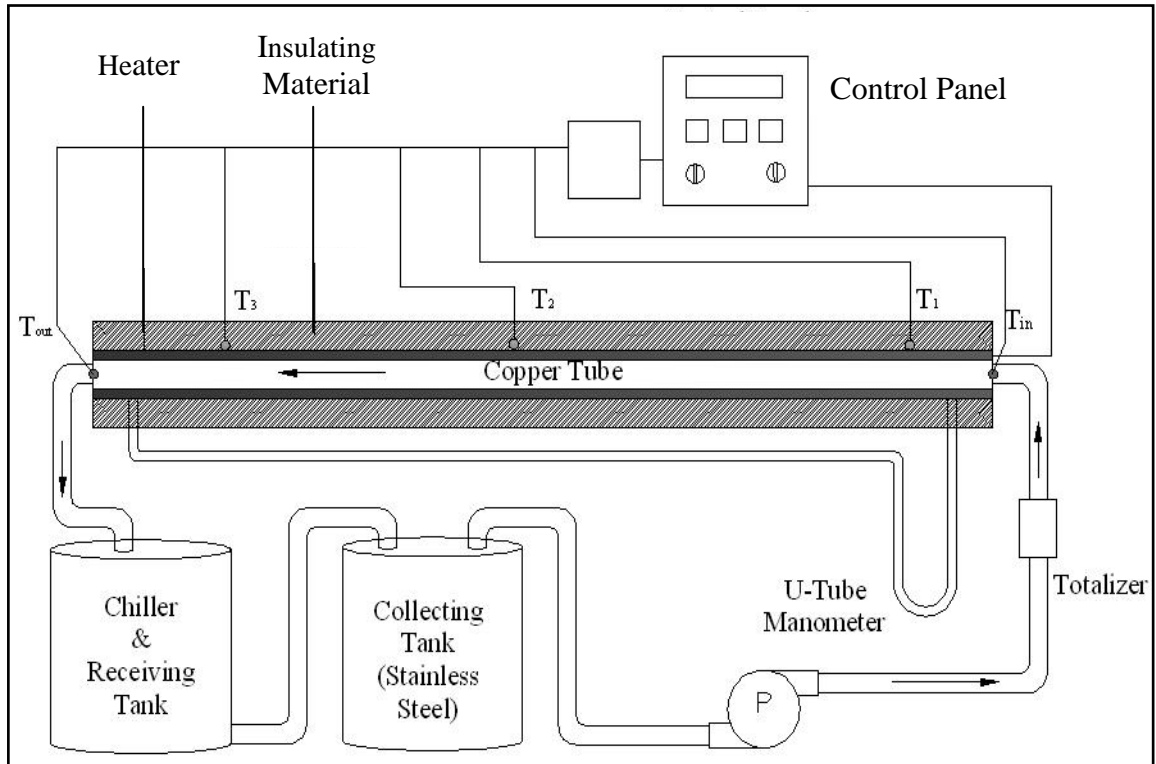
Figure 3.2: Experiment Schematic Diagram

A totalizer is located before working fluid enters the test section to determine the flow rate of the working fluid in the test section. When the system attains steady state, the temperatures at different locations, electric heat input and the flow rate is noted. The provision of chiller between the test section and the collecting tank helped to achieve steady state condition faster. U-tube manometer which fixes on the test section is helped to measure pressure drop when working fluid flow through a tube.

Experiments are initially conducted by using water and checked for consistency of results. The experiment is repeated with nanofluid at different parameters and heat transfer coefficients estimated. The assumptions are made in the analysis for estimation of convective HTC is there is no loss to environment and Newton's convective law is applicable to nanofluids in the nanofluids range tested.

3.6   RUNNING EXPERIMENT

In the experiment section, sample of nanofluids that were prepared in the pre-experiment which is Al_2O_3 dillute by water as a based fluid at three volume concentration 0.02%, 0.05% and 0.5%. Step by step of running experiment are as follow:-

1. Sample one of nanofluids is placed in the collecting tank before experiment is running.
2. Power supply is on to operate the heaters before circulating pump start to force the flow through the test section.
3. Circulating pump is operated based on desired Reynolds number with estimate from totalizer apparatus.
4. Volume flow rate, pressure drop along the test section and temperature difference on the test section is noted when temperature indicator on control panel is constant.
5. Experiment is running again with varies the Reynolds number for sample one starting with 4,000, 5,000, 7,000, 9,000, 10,000, 12,000, 13,500, 15,000, 17,000, 18,000, 19,000 and 20,000 .
6. When the experiment completed for sample one, collecting tank, chiller and test section need to flask before placed the other sample to make sure no nanofluids sample one is left inside.
7. The step 1 to 6 is repeated for another sample of nanofluids.

3.7   ANALYSIS

In the post-experiment section, data are going to analyze using circumstances equation to get the HTC value of the nanofluids sample. Analysis flow to determine HTC from experiment data have shown in the next sub chapter.

3.7.1 Desired Reynolds Number

Based on the assumptions state from previous section, condition of the experiment is assumed:

     i.   There is no heat loss to environment.

    ii.   Newton's convective law is applicable to nanofluids in the nanofluid range tested.

Desired Reynolds number is calculated from Eq. 2.25 while, mass flow rate is measured from totalizer during experiment conducted.

3.7.2 Experimental Heat Transfer Coefficient

Heat transfer coefficient (HTC) of experiment is calculated from Newton's law of cooling in Eq. 2.1. Arrangement from that equation will resulted of new equation of HTC experiment as shown in Eq. 3.1.

$$h_{exp} = \frac{\dot{Q}}{A_s(T_w - T_b)_{avg}}$$
(3.1)

Rate of energy is assume to be same as energy supplied since assumption of no heat losses to the environment have earlier made in this study and calculated by Eq. 3.2

$$\dot{Q} = V \times I \text{ (energy supplied)} = \dot{m}C_P(T_e - T_i)$$
(3.2)

Where,

        V = Voltage supplied to the heater

        I = Current supplied to the heater

A_s is defined as $A_s = \pi DL$ and T_w and T_b is determined by using Eq. 3.3 and Eq. 3.4, respectively.

$$T_{w\text{(avg)}} = \frac{T_1 + T_2 + T_3}{3} \tag{3.3}$$

$$T_b = \frac{T_i + T_e}{2} \tag{3.4}$$

3.7.3 Experimental Nusselt Number

Experiment Nusselt number is calculate from Eq. 2.21.

$$Nu_{exp} = \frac{h_{exp}D}{k}$$

Significant of Nusselt number to the heat transfer, when Nusselt number is higher, it represents very good heat transfer in convection situation. Since heat transfer coefficient, h is nominator in Nusselt number equation thus, high value of HTC represent very good heat transfer.

3.8 EXPERIMENT VERIFICATION

The result obtained from the experiment need to verify with the previous research result in literature and numerical study result to validate the result is in considerable range. Normally, average deviation below than 10% is considerably acceptable for experimental result.

3.9 EXPERIMENT APPARATUS

3.9.1 Circulating Pump

A circulation pump is used as an external means to force a fluid flow through a plain tube. Since the experiment is design in a close circuit, this type of pump is very suitable because the amount of effort required to overcome the force of friction within the piping system is significantly less than other types of pumping systems. An electric motor with capacity of 0.5 horse power is used to drive the circulation pump with

variable speed. Figure 3.3 shows the circulating pump used in this experiment with electric motor.
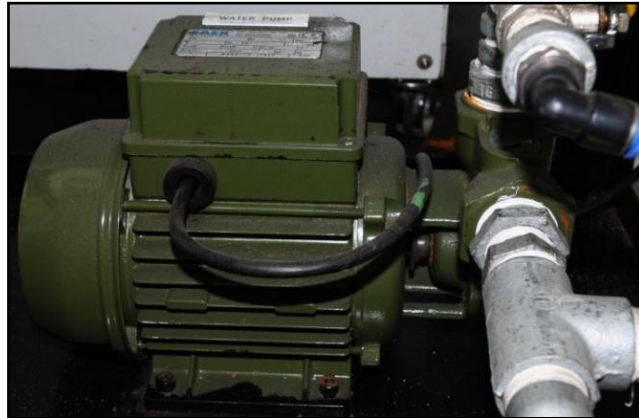
Figure 3.3: Circulating Pump with Electric Motor

3.9.2 Totalizer

Totalizer is placed after circulating pump to measure the volumetric flow rate of the fluid flow through the tube. It also designs to be used primarily with mass flow meters and mass flow controllers. It is one of the important instruments to define the desired parameters in this experiment. Digital type of totalizer is used to emphasize the accuracy in this experiment as shown in Figure 3.4.

Figure 3.4: Totalizer

3.9.3   Heater

Two nichrome heaters of 20 gauge having a resistance of 53.5 Ω per meter length and 1000 W maximum electrical rating is wrapping to the copper tube (plain tube) and subjected to entire test section to be constant heat flux boundary condition.

3.9.4   Control Panel

Control panel is used to control the power supply to the heater and to monitor the temperature measured for entire test section. All thermocouple is connected to the control panel as a center of monitoring experiment as shown in Figure 3.5.

Figure 3.5: Control Panel

3.9.5   Insulating Material

In order to minimize heat loss to the atmosphere, rock wool insulation is fixing in between the test section and the outer casing. Rock wool is used since their ability to partition air makes it excellent heat insulator and sound absorber. Table 3.1, show that typical insulator and their range of temperature can withstand.

Table 3.1: Insulator and Maximum Temperature Withstand

Material	Temperature (^{o}C)
Glass Wool	230-250
Stone/rock Wool	700-850
Ceramic Fibre Wool	1200

Source: MacDonald (2004)

3.9.6 Thermocouples

Five thermocouples K- type is provided to the test section in this experiment as shown in Figure 3.6 and three are brazed to the surface at distances of 0.375, 0.75 and 1.125m from the entry and the other two is located at the inlet and outlet test section to measure temperature of working fluid at that stages. All these thermocouples have 0.1^{o}C resolution and need to calibrate before fixing them at specified locations.
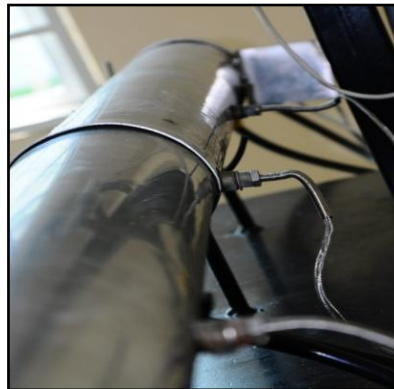
Figure 3.6: Thermocouple

3.9.7 Chiller and Receiving Tank

Chiller is used to cool the fluid which is heated in the test section and helped the fluid achieving steady state condition faster before go to collecting tank. The function of chiller is something like radiator in car to cool down the working fluid but in this

experiment, two different tanks is used to allowed fluid achieve steady state faster. Figure 3.7 have shown the chiller that was used in this experiment.

Figure 3.7: Chiller

3.9.8 Collecting Tank

Fluid that was flowing through a chiller and receiving tank are expected to achieve steady state condition of the fluid. Collecting tank also known as a storage tank is function to supply enough capacity of steady state fluid which is suction by circulating pump to the test section. The stainless steel tank shown in Figure 3.8 with capacity of 30 liter was used in this experiment to make sure fluids are enough for circulating.

Figure 3.8: Collecting Tank

3.9.9 U-Tube Manometer

U-tube manometer is fixing at the test section to measure the pressure drop of the fluid flow through a plain tube during the experiment running. Mercury is used in U-tube manometer since high pressure is predicted to obtain high Reynolds number. The concept of pressure measurement in U-tube manometer is when the legs of manometer are connected to separate sources of pressure, the liquid will rise in the leg with the lower pressure and drop in the other leg. The difference between the levels as Figure 3.9 shown is a function of the applied pressure and the specific gravity of the pressurizing and fill fluids.

Figure 3.9: U-Tube Manometer

Arrangement of the experiment set up had shown in Figure 3.10 and the functions of each apparatus have summarized in Table 3.2.

Figure 3.10: Apparatus Arrangement

Description:-

1. Circulating Pump
2. Totalizer
3. Control Panel
4. Chiller and Receiving Tank
5. Collecting Tank
6. U tube Manometer
7. Test Section (consist of 19mm inner diameter copper tube with 1.5m length, heater, insulator, thermocouples and stainless steel cover).

Table 3.2: Summarize Function for Each Apparatus

No.	Apparatus	Function
1	Circulating Pump	To force nanofluid flow through a plain tube (test section) and regulate the speed into desired velocity.
2	Totalizer	To measure a flow rate flow through a test section.
3	Control Panel	To control the power supply to the heater and monitor the temperature for each thermocouple connected to the test section
4	Chiller and Receiving Tank	To cool the fluid which is heated in the test section and helped the fluid achieving steady state condition faster.
5	Collecting Tank	Stored fluid in steady state condition to supplied to the pump.
6	U-Tube Manometer	To measure pressure drop in the test section.
7	Thermocouples	To measure temperature at that location.
8	Insulator	To minimize heat loss to the atmosphere.
9	Heater	To supply heat for entire test section in constant heat flux condition.

3.10   EXPERIMENT PARAMETER

The Parameters in this experiment is shown in Table 3.3 with only two variables parameters which are volume concentration and Reynolds number.

Table 3.3: Important Parameter Investigations

Volume Concentration (%)	Reynolds Number	Heater (W)	D (m)	Length Test Section (m)
0.02	4,000	570	0.019	1.5
0.02	5,000	570	0.019	1.5
0.02	7,000	570	0.019	1.5
0.02	9,000	570	0.019	1.5
0.02	10,000	570	0.019	1.5
0.02	12,000	570	0.019	1.5
0.02	13,500	570	0.019	1.5
0.02	15,000	570	0.019	1.5
0.02	17,000	570	0.019	1.5
0.02	18,000	570	0.019	1.5
0.02	19,000	570	0.019	1.5
0.02	20,000	570	0.019	1.5
0.1	4,000	570	0.019	1.5
0.1	5,000	570	0.019	1.5
0.1	7,000	570	0.019	1.5
0.1	9,000	570	0.019	1.5
0.1	10,000	570	0.019	1.5
0.1	12,000	570	0.019	1.5
0.1	13,500	570	0.019	1.5
0.1	15,000	570	0.019	1.5
0.1	17,000	570	0.019	1.5
0.1	18,000	570	0.019	1.5
0.1	19,000	570	0.019	1.5
0.1	20,000	570	0.019	1.5

Table 3.3: Continued

Volume Concentration (%)	Reynolds Number	Heater (W)	D (m)	Length Test Section (m)
0.5	4,000	570	0.019	1.5
0.5	5,000	570	0.019	1.5
0.5	7,000	570	0.019	1.5
0.5	9,000	570	0.019	1.5
0.5	10,000	570	0.019	1.5
0.5	12,000	570	0.019	1.5
0.5	13,500	570	0.019	1.5
0.5	15,000	570	0.019	1.5
0.5	17,000	570	0.019	1.5
0.5	18,000	570	0.019	1.5
0.5	19,000	570	0.019	1.5
0.5	20,000	570	0.019	1.5

CHAPTER 4

RESULTS AND DISCUSSION

4.1   INTRODUCTION

This chapter will present the experiment analysis result from the beginning until the end of the experiment. All evaluated data then being calculated then present as non-dimensionless result and graph. It then being discuss with the relationship of enhancement heat transfer when different nanofluids volume concentration were used.

In this study, water, and Nanofluids Aluminum oxide/water with 0.02%, 0.1% and 0.5% volume concentration are tested in experiment apparatus. The purpose of testing water is to verify accurate knowledge that the experiment data is consistent with analytical solution and proper comparison can be made between water and nanofluids.

The thermo physical properties needed for data analysis are specific heat, density, thermal conductivity and dynamic viscosity. These properties are temperature-dependent and vary with the type and volume concentrations.

4.2   THERMOPHYSICAL PROPERTIES STUDY

Thermophysical properties used in this study are predicted by using correlation that has developed by other researchers. Thus, result obtained in this study is depending to the accuracy of correlation used. The correlation used to predict water properties is different from nanofluid properties.

4.2.1   Determination of Water Properties

The regression equations by Azmi et al. (2010) in Eq. (2.26) to Eq. (2.29) are used to predict properties of water. The result obtained was compared with standard properties of saturated water in Appendix A as shown in Table 4.1.

Comparison graph was plotted as shown in Figure 4.1 to 4.4 and found close agreement between correlation equation and properties of saturated water with average deviation less than 1.1 %. This implies that regression equations are valid to predict thermophysical properties of water.

Table 4.1: Thermophysical properties of water estimation by regression equations

	Bulk Temperature, $T_b(^oC)$	Density, ρ (Kg/m^3)	Specific Heat, C_p $(J/Kg.K)$	Thermal Conductivity, k $(W/m.K)$	Dynamic Viscosity, μ 10^{-3} (Kg/ms)
Properties of	30.0	996.00	4178.0	0.6150	0.798
Saturated	32.5	995.00	4178.0	0.6190	0.759
Water	35.0	994.00	4178.0	0.6230	0.720
(Appendix A)	37.5	993.05	4178.5	0.6270	0.687
	40.0	992.10	4179.0	0.6310	0.653
	42.5	991.10	4179.5	0.6340	0.625
Regression	30.0	995.68	4178.26	0.6150	0.800
Equation	32.5	994.90	4177.98	0.6190	0.755
(Azmi et al.,	35.0	994.06	4177.93	0.6229	0.714
2010)	37.5	993.18	4178.05	0.6266	0.676
	40.0	992.25	4178.34	0.6303	0.641
	42.5	991.27	4178.75	0.6338	0.610
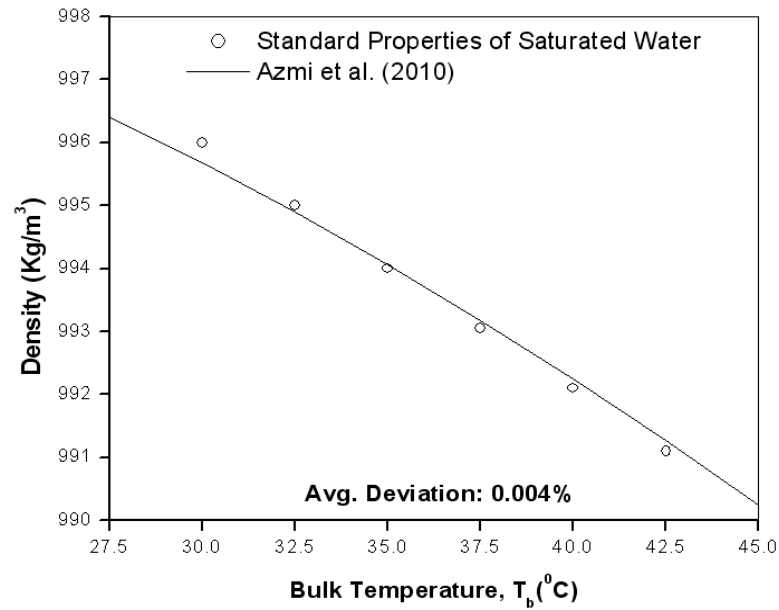
Figure 4.1: Comparison of density between standard properties of saturated water and regression equation by Azmi et al. (2010)
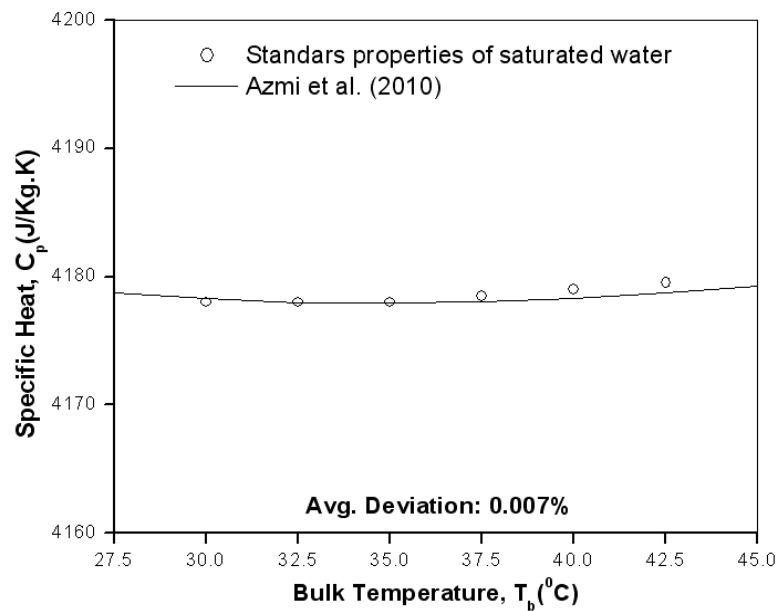
Figure 4.2: Comparison of specific heat between standard properties of saturated water and regression equation by Azmi et al. (2010)
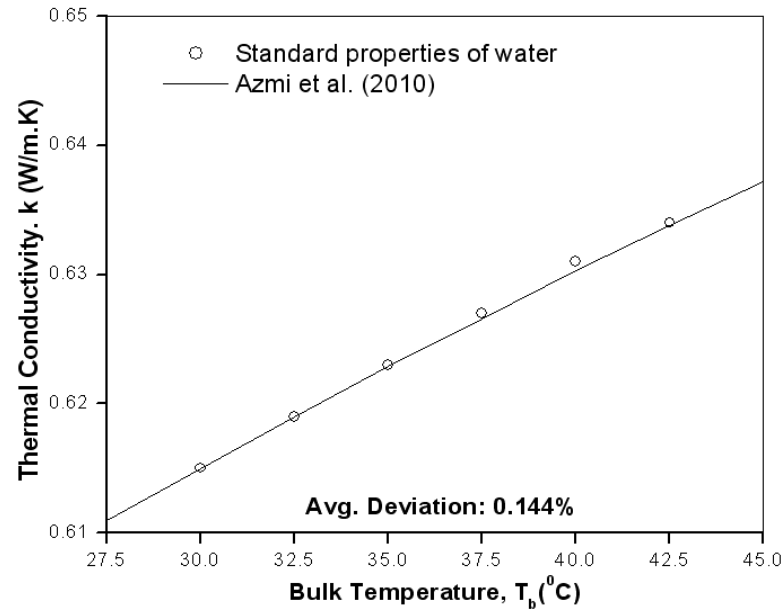
Figure 4.3: Comparison of thermal conductivity between standard properties of saturated water and regression equation by Azmi et al. (2010)
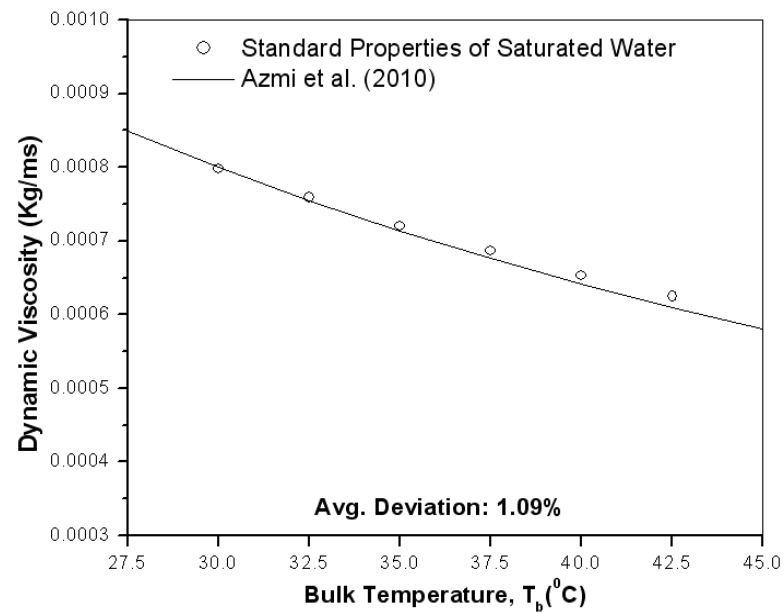
Figure 4.4: Comparison of dynamic viscosity between standard properties of saturated water and regression equation by Azmi et al. (2010)

4.2.2 Determination of Nanofluids Properties

In this experiment, correlation used to predict the thermophysical properties of nanofluid has developed by another study. Thus, the accuracy of the properties is depend to the regression equation that has developed.

Regression equation that is used to predict the thermophysical properties of nanofluid in this study is shown in Eq. 4.1 to Eq. 4.4.

For Dynamic Viscosity (Azmi et al., 2010),

$$\frac{\mu_{nf}}{\mu_w} = 0.9042 + 0.1245 \times \emptyset + 0.6436 \times \left(\frac{d_p}{d_{max}}\right) - 0.08445 \times \left(\frac{T_b}{T_{max}}\right) \qquad (4.1)$$

For Thermal Conductivity (Azmi et al., 2010),

$$\frac{k_{nf}}{k_w} = 0.9808 + 0.0142 \times \emptyset + 0.2718 \times \left(\frac{T_b}{T_{max}}\right) - 0.1020 \times \left(\frac{d_p}{d_{max}}\right) \qquad (4.2)$$

For Density, (Eq. by Taufiq, 2010)

$$\frac{\rho_{nf}}{\rho_w} = 0.9988 + 0.03485\emptyset + 0.002217\left(\frac{T_b}{70}\right) \qquad (4.3)$$

For Specific Heat, (Eq. by Taufiq, 2010)

$$\frac{C_{p_{nf}}}{C_{p_w}} = 0.9977 - 0.03344\emptyset - 0.001111\left(\frac{T_b}{70}\right) \qquad (4.4)$$

The validation of the regression equation developed by Azmi et al., (2010) has shown in Figure 4.5 and Figure 4.6. While, regression equation developed by Taufiq, (2010) have been validated as shown in Figure 4.7 and Figure 4.8. It can be seen, the

present regression equation is in close agreement with previous researchers result that have been compared in their study.
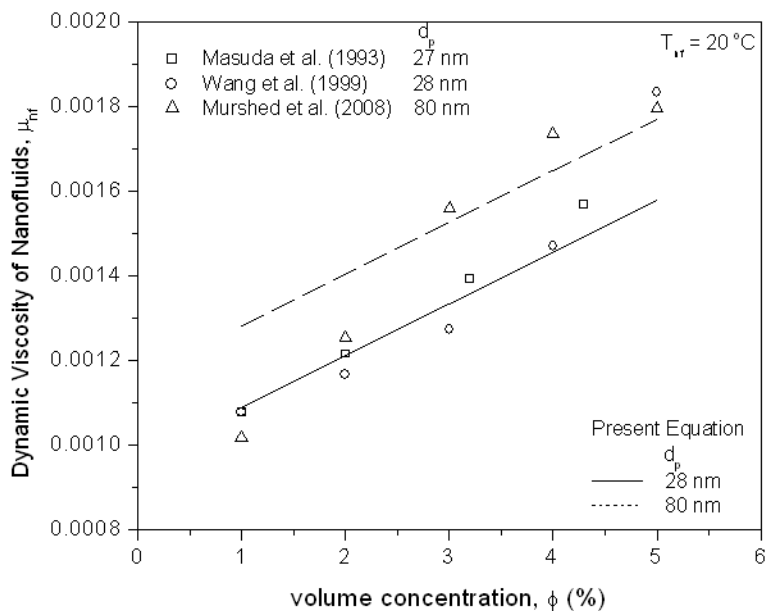
Figure 4.5: Comparison between regression equation and experiment data for dynamic viscosity
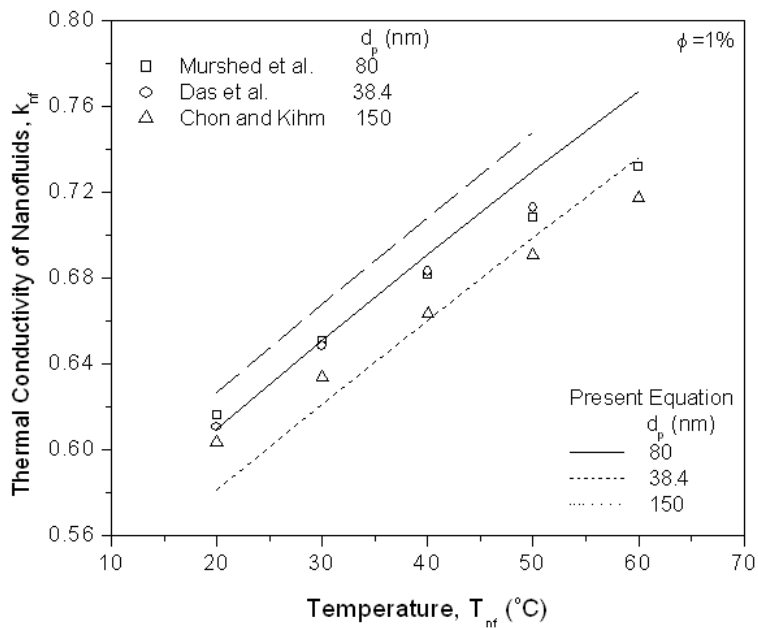
Figure 4.6: Comparison between regression equation and experiment data for thermal conductivity
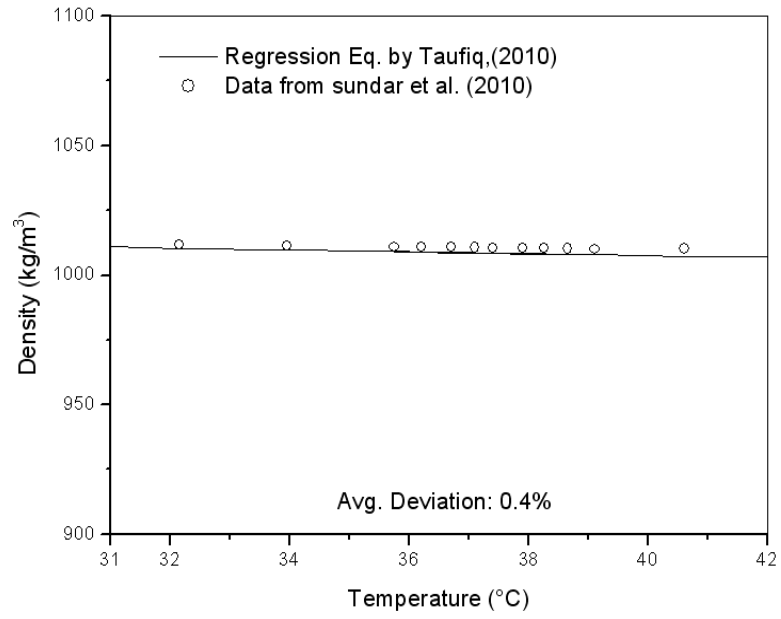
Figure 4.7: Comparison between regression equation and experiment data for density
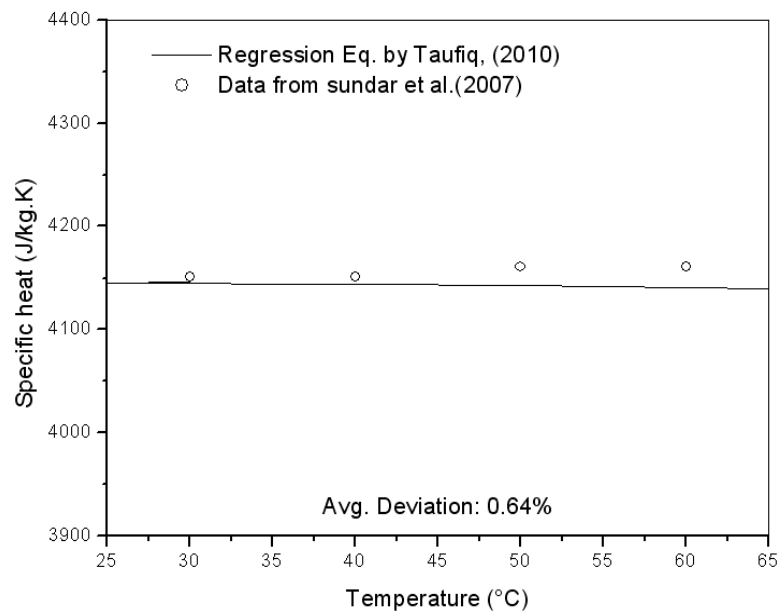
Figure 4.8: Comparison between regression equation and experiment data for specific heat

4.3   CALIBRATION TEST

The accuracy and reliability of the experimental system were tested before measuring the convective heat transfer coefficient of nanofluids. This was carried out by using water as the working fluid and it is runs for different flow rates, which give a wide range of Reynolds number. The experimental results of the convective heat transfer coefficient were analyzed by using FORTRAN to transform crude value of experiment result to the final experiment value. Then, final values of experiment were compared with the predicted values obtained from Gnielinski Eq. (Gnielinski, 1976) and Dittus and Boelter (1930) equations.

Details of calculated results from Gnielinski equation, Dittus-Boelter equation and experiment are present in Table 4.2, 4.3 and 4.4, respectively. Comparison based on Nusselt number calculated is shown in Figure 4.9. The Ditus-Boelter equation predicts the experimental Nusselt number values for water better compared to Gnielinski equation. The deviation between Gnielinski equation and Dittus-Boelter equation is found less than 7.35% and the deviation between Dittus-Boelter equation and present experiment data is found less than 4.4%. This implies that the precision of the experimental system is accepted with average deviation below than 10% when compared to both equations.

Table 4.2: Data Contribution by Using Gnielinski Equation

V = 190V & I = 3 A							
Run	$\dot{m}$, (Kg/s)	Avg. T_w (°C)	T_b (°C)	f	Pr	Re	h (W/m^2.K)	Nu
1	0.03647	72.96	39.70	0.0118	4.2802	3787.93	899.95	27.15
2	0.04638	70.96	38.35	0.0110	4.4166	4682.87	1140.06	34.50
3	0.05641	69.00	37.45	0.0104	4.5115	5587.42	1371.74	41.60
4	0.06573	67.03	36.35	0.0100	4.6320	6357.69	1567.64	47.66
5	0.07630	65.43	35.45	0.0096	4.7344	7236.10	1784.52	54.38
6	0.08966	62.83	34.90	0.0091	4.7987	8400.45	2059.26	62.83
7	0.10445	67.26	37.65	0.0086	4.4901	10390.18	2454.59	74.40

Table 4.2: Continued

			V = 190V & I = 3 A					
Run	$\dot{m},$	*Avg. T_w*	T_b (°C)	*f*	*Pr*	*Re*	*h*	*Nu*
	(Kg/s)	**(°C)**					**(W/m^2.K)**	
8	0.14325	59.89	36.50	0.0079	4.5656	12470.26	3204.26	97.39
9	0.16256	56.58	35.35	0.0077	4.6152	13901.02	3530.33	107.60
10	0.18889	52.42	33.20	0.0075	4.5656	15382.87	3920.06	120.11
11	0.22495	48.92	31.25	0.0072	4.6152	17036.53	4454.12	137.15
12	0.14325	59.89	36.50	0.0079	5.2602	19404.75	3204.26	97.39

Table 4.3: Data Contribution by using Dittus-Boelter Equation

				V = 190V & I = 3 A				
Run	$\dot{m},$	*Avg. T_w*	T_b	*Pr*	*Re*	Nu_w	h_{exp}	Nu_{exp}
	(Kg/s)	**(°C)**	**(°C)**			**(Theory)**	**(W/$m^2.K$)**	
1	0.03647	72.96	39.70	4.2802	3787.93	30.17	994.27	29.99
2	0.04638	70.96	38.35	4.4166	4682.87	34.78	1189.30	35.99
3	0.05641	69.00	37.45	4.5115	5587.42	39.44	1378.57	41.80
4	0.06573	67.03	36.35	4.6320	6357.69	43.47	1540.78	46.85
5	0.07630	65.43	35.45	4.7344	7236.10	47.62	1720.12	52.41
6	0.08966	62.83	34.90	4.7987	8400.45	53.11	1946.06	59.38
7	0.10445	67.26	37.65	4.4901	10390.18	71.42	2261.19	68.54
8	0.12726	62.63	36.95	4.5656	12470.26	81.34	2629.77	79.84
9	0.14325	59.89	36.50	4.6152	13901.02	88.44	2877.83	87.47
10	0.16256	56.58	35.35	4.7460	15382.87	97.03	3147.05	95.92
11	0.18886	52.42	33.20	5.0059	17036.53	107.32	3470.05	106.32
12	0.22495	48.92	31.25	5.2602	19404.75	116.2	3908.51	120.35

Table 4.4: Experiment Data Distribution for Water

				V = 190V & I = 3 A				
Run	$\dot{m}$,	**Avg. T_w**	T_b	**Pr**	**Re**	Nu_w	h_{exp}	Nu_{exp}
	(Kg/s)	**(°C)**	**(°C)**			**(Theory)**	**(W/m^2. K)**	
1	0.03647	72.96	39.70	4.2802	3787.93	30.17	1000.11	30.17
2	0.04638	70.96	38.35	4.4166	4682.87	34.78	1149.34	34.78
3	0.05641	69.00	37.45	4.5115	5587.42	39.44	1300.59	39.44
4	0.06573	67.03	36.35	4.6320	6357.69	43.47	1429.74	43.47
5	0.07630	65.43	35.45	4.7344	7236.10	47.62	1562.83	47.62
6	0.08966	62.83	34.90	4.7987	8400.45	53.11	1740.67	`53.11
7	0.10445	67.26	37.65	4.4901	10390.18	71.42	2356.29	71.42
8	0.12726	62.63	36.95	4.5656	12470.26	81.34	2679.13	81.34
9	0.14325	59.89	36.50	4.6152	13901.02	88.44	2909.86	88.44
10	0.16256	56.58	35.35	4.7460	15382.87	97.03	3183.63	97.03
11	0.18886	52.42	33.20	5.0059	17036.53	107.32	3502.59	107.32
12	0.22495	48.92	31.25	5.2602	19404.75	116.2	3773.65	116.20
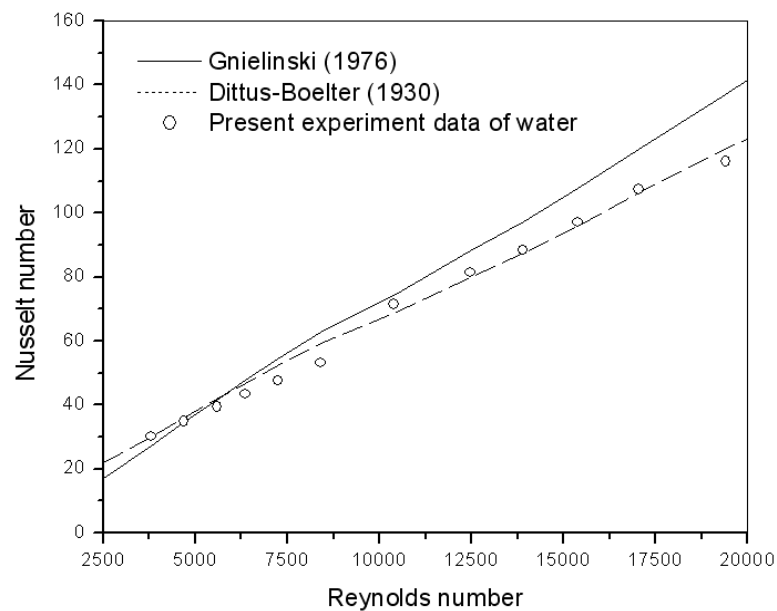
Figure 4.9: Comparison between experimental Nusselt number for water and that Theoretical calculated

The measured Nusselt number is compared to that predicted Nusselt number of the Gnielinski equation as defined in Eq. 2.19. Properties of the water are determined from Azmi et al. (2010) regression equation. The resulting plot is shown in Figure 4.10. It can be seen in the figure that Nusselt number is effectively predicted by the Gnielinski equation within deviation of ±10%.
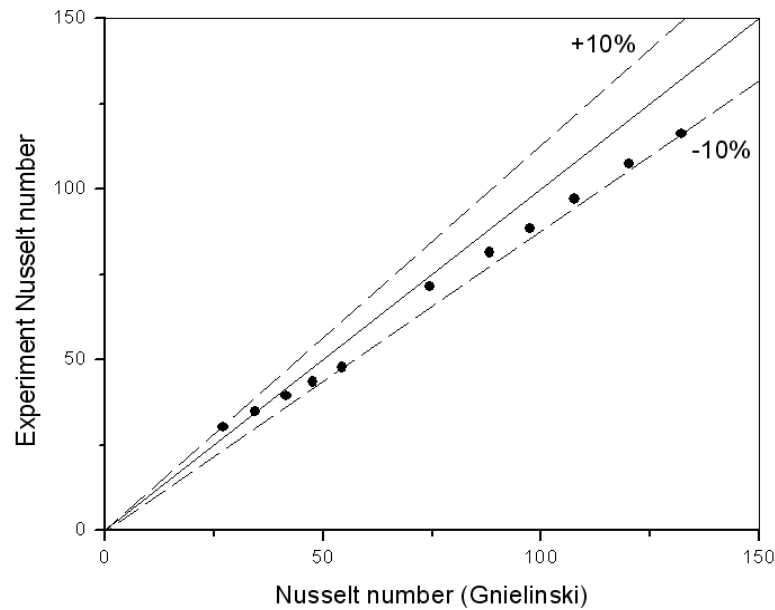
Figure 4.10: Nusselt number comparison for water

4.4 NANOFLUIDS TEST

4.4.1 Experiment of Alumina Al$_2$O$_3$/Water with Different Volume Concentration

Experiment of Alumina dilute by water at three different volume concentrations which is 0.02%, 0.10% and 0.50% was conducted in this study. The results of each experiment are present afterword.

1.   0.02% Volume Concentrations

Results of the experiment Alumina with $\emptyset = 0.02\%$ is shown in Table 4.5 followed by comparison of Nusselt number with water as shown in Figure 4.11 with maximum enhancement of 6.07% at Reynolds number 18,000 was observed.

Table 4.5: Experiment Data Distribution for (Al$_2$O$_3$/Water) with $\emptyset = 0.02\%$

					V = 190V & I = 3 A				
Run	$\emptyset$	$\dot{m}$,	*Avg. T_w*	T_b	*Pr*	*Re*	Nu_w	$h_{nf,\,exp}$	$Nu_{nf,\,exp}$
	(%)	**(Kg/s)**	**(°C)**	**(°C)**			**(theory)**	**(W/m^2.K)**	
1	0.02	0.03647	71.40	39.95	4.0763	3593.50	31.11	1090.62	29.78
2	0.02	0.04638	68.56	38.50	4.2440	4426.94	36.01	1290.94	35.55
3	0.02	0.05641	66.56	37.55	4.3594	5271.13	40.81	1463.60	40.53
4	0.02	0.06573	64.50	36.45	4.4987	6049.46	45.41	1633.58	45.53
5	0.02	0.07630	62.70	35.55	4.6174	6815.57	49.68	1800.39	50.45
6	0.02	0.08966	61.00	35.05	4.6853	8203.41	57.33	2022.34	56.84
7	0.02	0.10445	65.66	37.65	4.3470	9699.70	71.57	2496.12	69.07
8	0.02	0.12726	61.02	37.00	4.4283	11671.89	82.64	2910.06	80.84
9	0.02	0.14325	58.48	36.65	4.4729	13044.94	90.80	3201.00	89.11
10	0.02	0.16256	55.00	35.50	4.6242	14385.42	93.65	3345.34	93.77
11	0.02	0.18886	50.75	33.25	4.9412	15852.02	108.08	3874.09	110.08
12	0.02	0.22495	47.46	31.40	5.2242	17754.62	120.47	4304.53	123.71
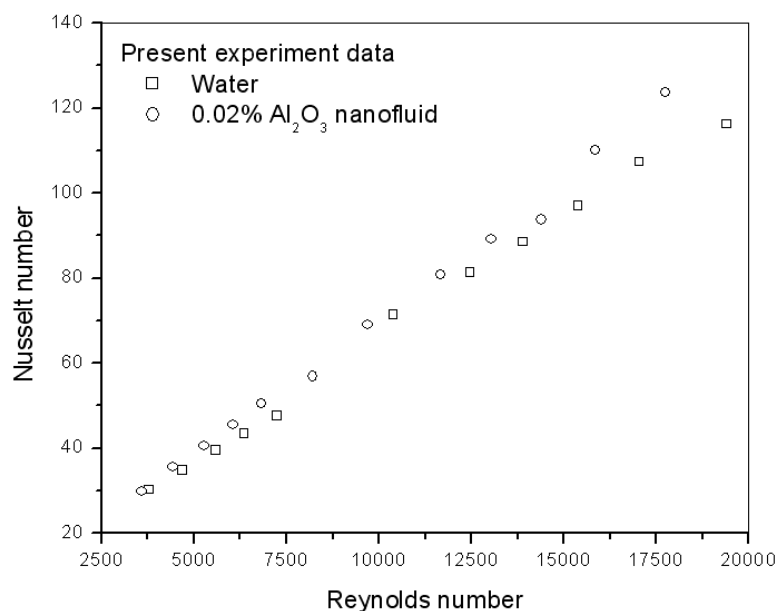
Figure 4.11: Comparison of Nusselt number of Alumina 0.02% volume concentration with water

2.   0.10% Volume Concentration

Results of experiment by using Alumina with $\emptyset = 0.10\%$ is shown in Table 4.6 followed by comparison of Nusselt number with water as shown in Figure 4.12 with the maximum enhancement of 17.70% at Reynolds number 7,500 was observed.

Table 4.6: Experiment Data Distribution for (Al_2O_3/Water) with $\emptyset = 0.10\%$

V = 190V & I = 3 A									
Run	**$\emptyset$**	**$\dot{m}$,**	**$Avg.\ T_w$**	**T_b**	**Pr**	**Re**	**Nu_w**	**$h_{nf,\ exp}$**	**$Nu_{nf,\ exp}$**
	(%)	**(Kg/s)**	**(°C)**	**(°C)**			**(theory)**	**(W/$m^2.K$)**	
1	0.1	0.036585	69.33	40.10	4.0824	3581.00	31.06	1171.56	31.93
2	0.1	0.049916	66.43	38.60	4.2559	4727.42	37.63	1457.11	40.06
3	0.1	0.056572	64.93	37.65	4.3714	5245.19	40.69	1551.84	42.90
4	0.1	0.069965	62.66	36.55	4.5109	6327.21	46.72	1805.59	50.24
5	0.1	0.079989	59.90	35.65	4.6298	7085.82	50.98	2068.44	57.86
6	0.1	0.093225	58.56	35.15	4.9835	7788.73	58.85	2120.08	60.21
7	0.1	0.121416	58.33	38.05	4.3223	11358.84	60.28	2903.70	80.08
8	0.1	0.153023	56.76	37.45	4.3963	14124.05	75.60	3311.49	91.65
9	0.1	0.169757	55.26	36.95	4.4595	15492.26	86.58	3639.00	101.01
10	0.1	0.182826	53.36	35.95	4.5897	16307.95	98.54	3942.58	110.09
11	0.1	0.213267	49.93	33.65	4.9099	18030.16	106.41	4100.06	116.09
12	0.1	0.243398	47.53	31.75	5.1977	19665.80	123.06	4475.09	128.19
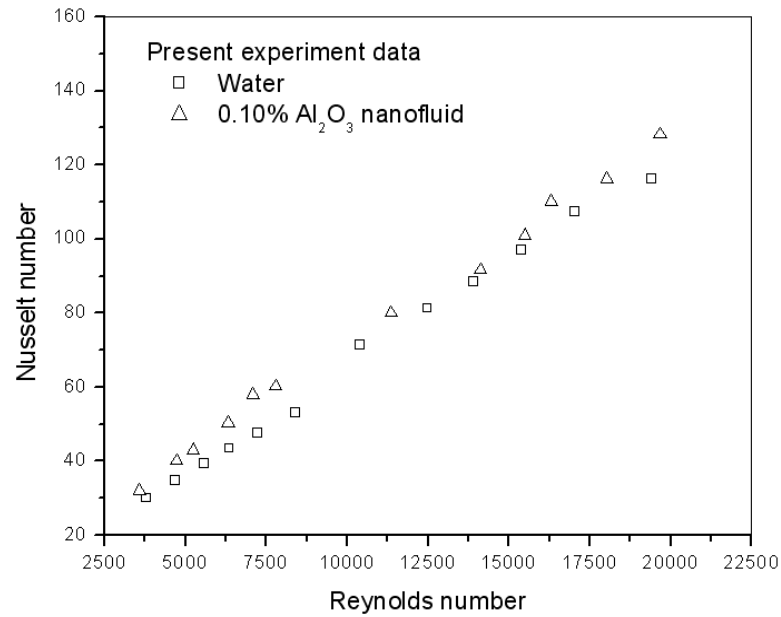
Figure 4.12: Comparison of Nusselt number of Alumina 0.10% volume concentration with water

3.   0.50% Volume Concentration

Results of experiment by using Alumina with $\emptyset = 0.50\%$ is shown in Table 4.7 followed by comparison of Nusselt number with water as shown in Figure 4.13 with maximum enhancement of 19.80% at Reynolds number 8,400 was observed.

Table 4.7: Experiment Data Distribution for (Al$_2$O$_3$/Water) with $\emptyset = 0.50\%$

				V = 190V & I = 3 A					
Run	$\emptyset$ (%)	$\dot{m}$, (Kg/s)	Avg. T_w (°C)	T_b (°C)	Pr	Re	Nu_w (theory)	$h_{nf, exp}$ (W/m^2.K)	$Nu_{nf, exp}$
1	0.5	0.037026	68.10	40.25	4.1763	3474.25	30.80	1219.32	33.03
2	0.5	0.047134	65.23	38.58	4.3737	4263.84	36.09	1459.35	39.92
3	0.5	0.057188	63.16	37.85	4.4643	5089.88	40.28	1655.77	45.48
4	0.5	0.070745	60.96	36.75	4.6060	6142.18	46.19	1925.20	53.23
5	0.5	0.080872	59.06	35.85	4.7268	6878.51	50.39	2136.11	59.38

Table 4.7: Continued

				V = 190V & I = 3 A					
Run	**∅**	**$\dot{m}$,**	**Avg. T_w**	**T_b**	**Pr**	**Re**	**Nu_w**	**$h_{nf, exp}$**	**$Nu_{nf, exp}$**
	(%)	**(Kg/s)**	**(°C)**	**(°C)**			**(theory)**	**(W/m^2.K)**	
6	0.5	0.097726	57.83	35.35	4.7958	8216.79	57.81	2354.06	65.63
7	0.5	0.122856	57.56	38.20	4.4205	11020.33	58.11	2932.19	80.38
8	0.5	0.154904	56.10	37.60	4.4959	13709.76	74.35	3399.33	93.51
9	0.5	0.171804	54.76	37.05	4.5667	15018.07	85.07	3696.67	102.02
10	0.5	0.184988	52.76	36.05	4.6996	15806.40	88.67	3696.30	102.62
11	0.5	0.215749	49.46	33.70	5.0338	17454.93	104.38	4154.54	116.98
12	0.5	0.246199	47.20	31.90	5.3119	19083.92	120.78	4529.97	128.96
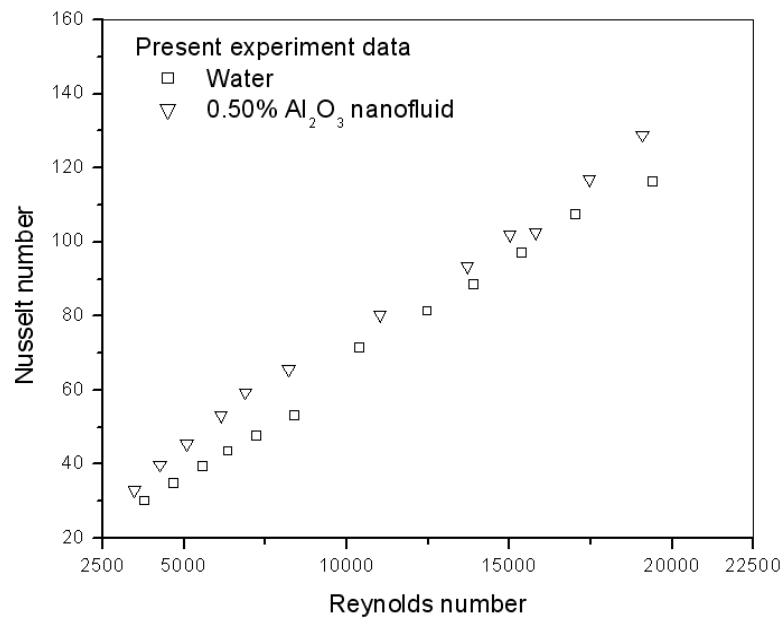
Figure 4.13: Comparison of Nusselt number of Alumina 0.50% volume concentration with water

4.4.2   Result Comparison for Different Volume Concentrations

From Figure 4.11 to Figure 4.13, experimental results are indicated that addition of small amount of nanoparticles to pure water improved the heat transfer performance significantly compared to pure water. However, increasing of small amount of volume concentrations in the small range studied in this work did not show much effect on heat transfer enhancement as shown in Figure 4.14.
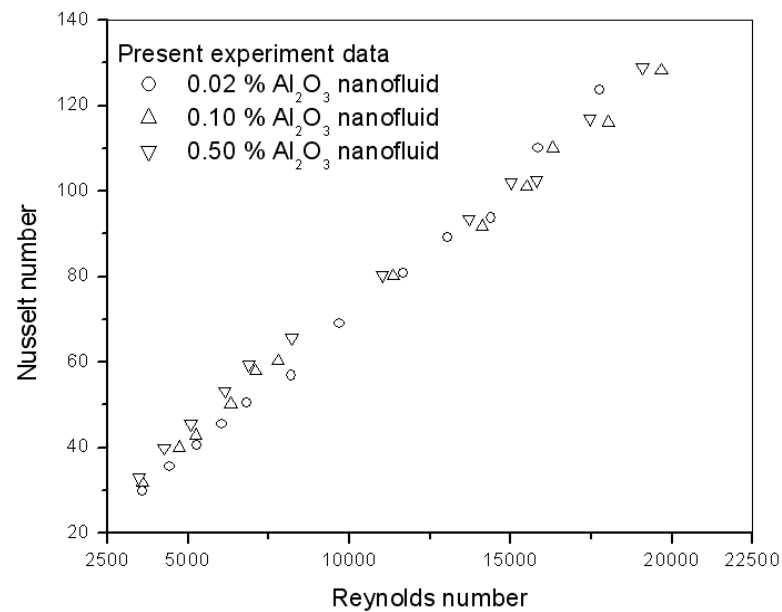
Figure 4.14: Comparison Nusselt number of nanofluid with different concentrations

While, Figure 4.15 and Figure 4.16 shown experimental results of heat transfer coefficient and Nusselt number of nanofluid with all volume concentration in the range of studied are indicated above the present experimental result of pure water which means, heat transfer rate are enhanced when nanofluid used as working fluid. The maximum value of 19.80% increased in heat transfer coefficient compared to pure water at Reynolds number 8,400 and 0.50% volume concentration was observed.
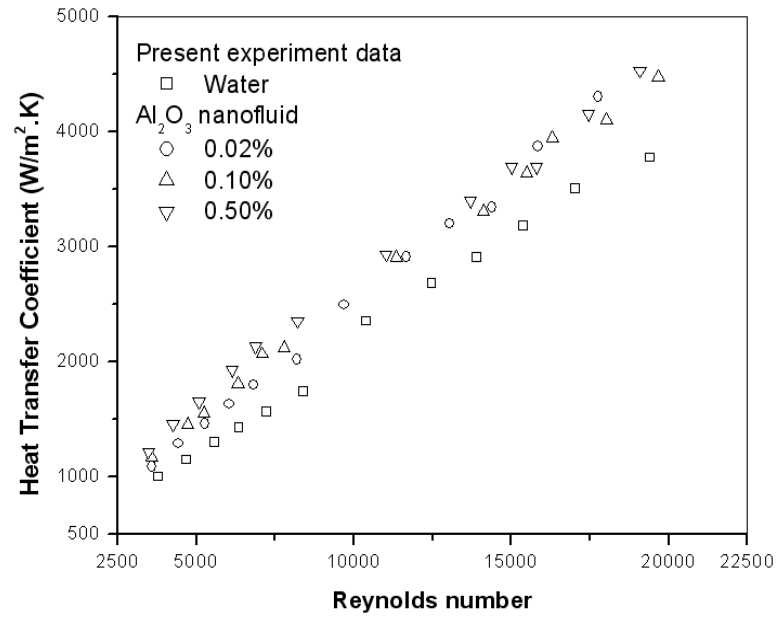
Figure 4.15: Comparison Heat Transfer Coefficient of nanofluid at different volume concentrations with water
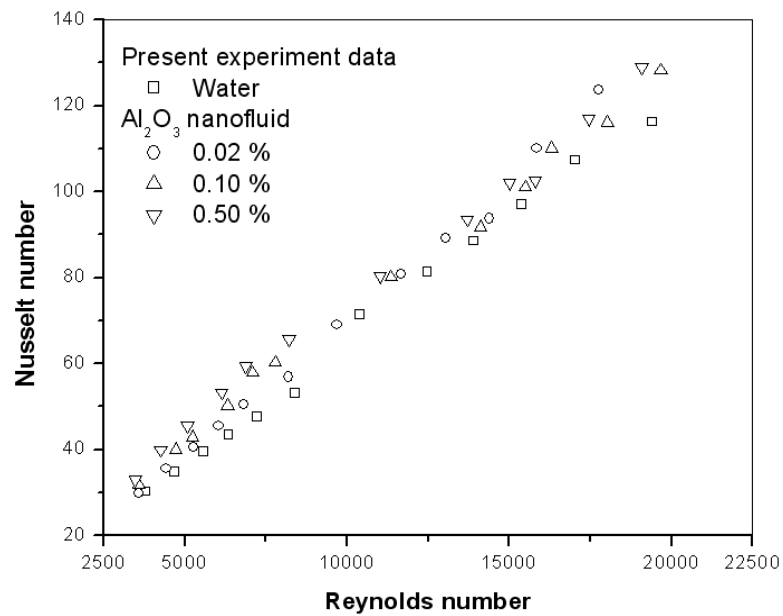
Figure 4.16: Comparison Nusselt number of nanofluid at different volume concentrations with water

Heat transfer rate found directly proportional to the velocity of the fluid flow through a tube as shown in Figure 4.17. When velocity of fluid flow increased, Nusselt number also increased and this behavior of fluid flow is observed for both nanofluid and pure water flow in a plain tube.
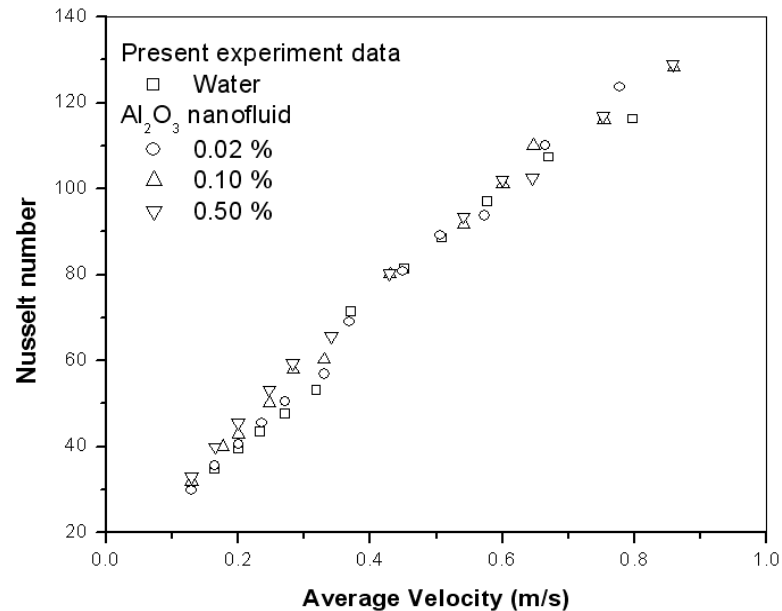
Figure 4.17: Effect of velocity to heat enhancement

4.4.3   Wall Temperature Effect

Comparison of wall temperature of the test section tube for nanofluid against water flow has shown in Figure 4.18. The wall temperature for nanofluid is significantly lower than the wall temperature for water. This could be due to the augmented thermal energy transfer from the wall to the nanofluid flowing in the tube in presence of naoparticles. Nanoparticles hit the wall and absorb thermal energy, lowering the wall temperature and mix back with the bulk of the fluid. The temperature difference between the wall and bulk of the nanofluid was lower than that of the temperature difference between wall and water. Maiga et al. (2004) also showed that the tube wall temperature decreased by suspending nanoparticles into water
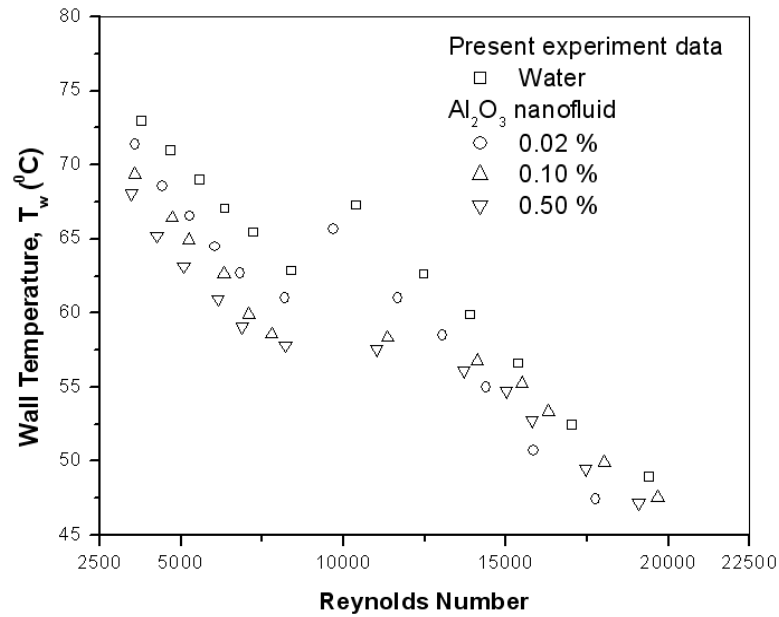
Figure 4.18: Effect of wall temperature of nanofluid and pure water versus Reynolds number

4.5   RESULT VALIDATION

Experiment result has been validated with comparison with previous literature result and numerical study conducted by Taufid, (2010) and present in the next sub-chapter.

4.5.1   Previous Research Result

Figure 4.19 shows the comparison of experimental Nusselt number with the prediction of Pak and Cho, (1998) and Maiga et al., (2006) correlations for different concentration in the range of studied. The experimental result found in close agreement with Pak and Cho correlation with maximum average deviation is 5.96% at 0.50% volume concentration, while Maiga's correlation is observed overestimates the value of Nusselt number for nanofluid in the range of studied.
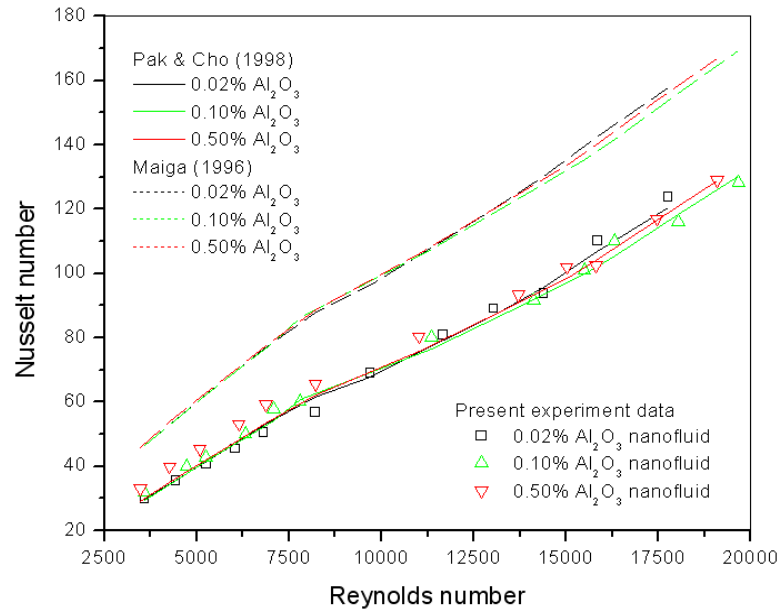
Figure 4.19: Comparison of experiment Nusselt number with proposed correlations for nanofluids at different concentration

4.5.2 Numerical Study Result

The present experiment result is validated by numerical study had done by Taufid, (2010) and result found consistent behavior as shown in Figure 4.20. The parity graph was constructed as shown in Figure 4.21 and found deviation is in considerable range with ±10% for all concentration in the range of studied. This implies that results from experiment are valid with small deviation observed when compared to numerical study.
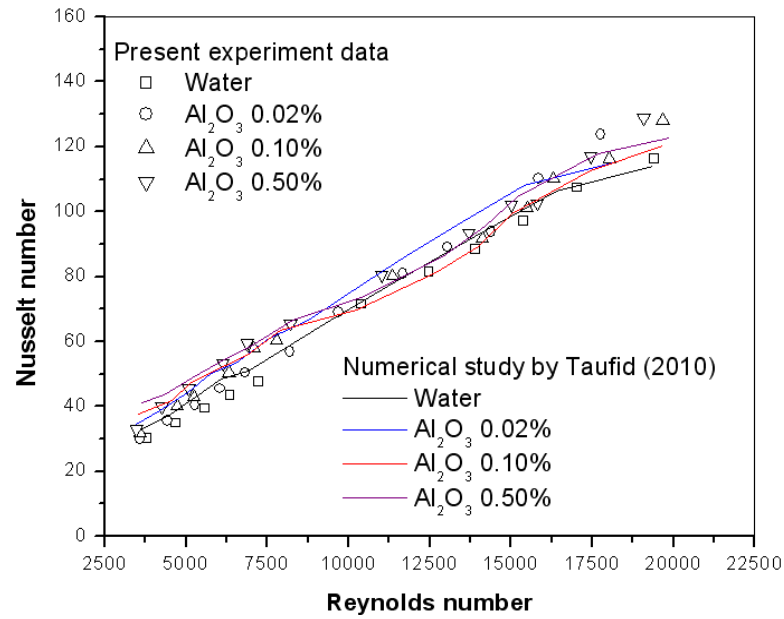
Figure 4.20: Comparison experiment data of Alumina and numerical study result by Taufid, (2010)
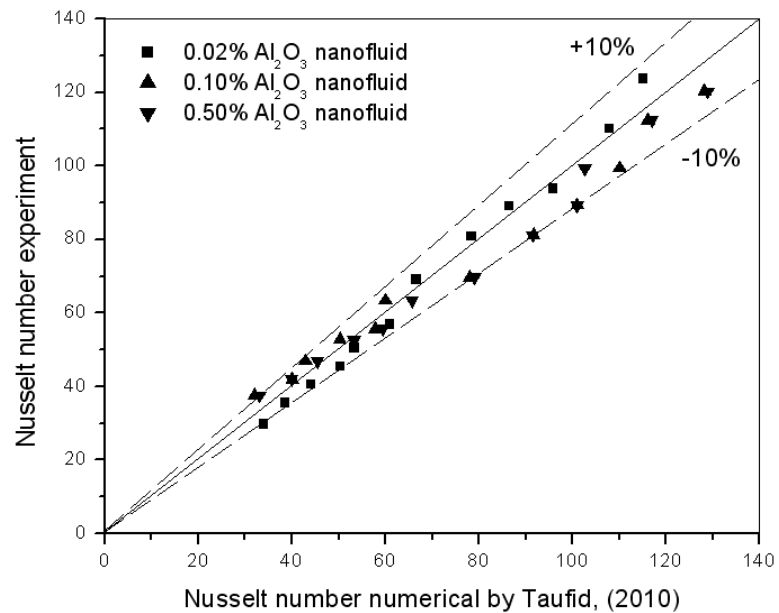
Figure 4.21: Nusselt number comparison for nanofluids with different concentration

CHAPTER 5

CONCLUSION AND RECOMMENDATIONS

5.1 CONCLUSION

The heat transfer coefficient of Alumina nanofluid with 0.02%, 0.10% and 0.50% volume concentration was investigated experimentally in fully develop turbulent region flowing through a plain tube. The maximum enhancement value of 19.8% increased in heat transfer coefficient compared to pure water for 0.50% volume concentration at Reynolds number of 8,400 was observed.

Experimental result is validated by previous result in the literature and found consistent behavior with considerable maximum average deviation from three volume concentrations is 5.96% when compared with Pak and Cho (1998) suggested correlation. While, comparison of experiment result with numerical study is found average deviation is less than 10% for all concentration.

As a conclusion, the overall characterization of nanofluids heat transfer coefficient can be conclude that the additional of small amount of nanoparticles will increased heat transfer performance of base fluid in the range of studied. The objectives of study have achieved with HTC determined from experimental found consistent with previous research result and numerical result.

5.2 RECOMMENDATIONS

In order to get more precision result during this study, recommendations and adjustment need to be arranged especially in experiment apparatus used during the experiment for example applied speed control motor to provide desired flow rate and large capacity of chiller to achieve steady state condition in testing fluid.

Then, thermophysical properties of nanofluids that was used in experiment should be determine by using experimental method compared to correlation that was obtained from previous researchers to optimum their accuracy of the results.

Various types of nanofluids with different concentration and nanoparticles size should be tested in heat transfer enhancement study and also their effect on pressure drop and clogging inside the tube.

Pressure drop of nanofluid flow need to investigate since convective heat transfer is link together with the pressure drop effect to optimum the required power pumping by motor in order to apply in industrial applications.

Lastly, future study should be directed to how to produce nanofluids with low cost and mass production since the nanoparticles available in the market is very expensive and almost impossible for commercialization.

REFERENCES

Azmi, W. H., Sharma, K.V., Sarma, P.K., and Rizalman Mamat. 2010. Influence of Certain Thermo-Physical Properties on Prandtl Number of Water Based Nanofluids, ,*National Conference in Mechanical Engineering Research and Postgraduate Students* (1st NCMER 2010), 26-27 MAY 2010, FKM Conference Hall, UMP, Kuantan, Pahang, Malaysia; pp. 502-515 ISBN: 978-967-5080-9501

Buongiorno, J. 2006. Convective heat transfer enhancement in nanofluids. *Heat and Mass Transfer Conference*. *HMT*-2006-C335.

Chon, C.H., Kihm, K.D., Lee, S.P., and Choi, S.U.S. 2005. Empirical correlation finding the role of temperature and particle size for nanofluid (Al_2O_3) thermal conductivity enhancement. *Applied physics Letters.* **87**: 1-3

Choi, S.U.S. 1995. Enhancing thermal conductivity of fluid with nanoparticles. In: Siginer, D.A, Wang, H.P. (Eds.), Developments and Applications of Non-Newtonian Flows, FED-V.231/MD-V.**66**. ASME, New York, pp. 99-105.

Chopkar, M., Das, P.K. and Manna, I. 2006. Synthesis and characterization of nanofluid for advanced heat transfer applications. *Scr. Mater.* **55**: 549–552.

Cengel, Y. A. 2006. *Heat and Mass Transfer: A Practical Approach* (3rd ed), *SI units*, New York: McGraw-Hill.

Das, S.K., Choi, S.U.S., Yu, W., and Pradeep, T. 2008. *Nanofluids: Science and Technology*, New York: John Wiley & Son, Inc.

Dittus, F. W. and Boelter, L.M.K. 1930. University of California Publications on Engineering 2, p. 433

Das, S.K., Putra, N., Theisen, P., and Roetzel, W. 2003. Temperature dependence of thermal conductivity enhancement for nanofluid. *Journal of Heat Transfer.* **125**: 567–574

Duncan, M.A., and Rouvray, D.H. 1989. Microclusters, *Sci. Am.*, Dec., pp. 110–115.

Duangthongsuk, W. and Wongwises, S. 2008. Effect of thermo-physical properties models on the prediction of the convective heat transfer coefficient for low concentration nanofluids. *International Communication in Heat and Mass Transfer*. **35**(10):1320-6.

Deventer, J. V., 2004. One dimensional modeling of a step-down ultrasonic densitometer for liquids. *Journal of Ultrasonic.* **42**: 309-314

Eastman, J.A., Choi, S.U.S., Li, S., Soyez, G., Thompson, L.J. and DiMelfi, R.J. 1999. Novel Thermal Properties of Nanostructure Materials. *Material Science Forum.* **312**: pp. 629-34.

Eastman, J.A., Choi, S.U.S., Li, S., Thompson, L.J. and Lee, S. 1997. Enhancement thermal conductivity through the development of nanofluids. *Fall meeting of the Materials Research Society (MRS)*, Boston, USA.

Fotukian, S.M. and Esfahany, M.N. 2010. Experimental investigation of turbulent convective heat transfer od dilute Al_2O_3/Water nanofluid inside circular tube. *International Journal of Heat and Fluid Flow*. **31**: 606-612.

Gnielinski, V., 1976. New Equation for Heat and Mass Transfer in Turbulent pipe and Channel Flow. *International Chemical Engineering*. **19**: pp. 359-368.

Godson, L., Raja, B., Mohan Lal, D., Wongwises, S., 2009. Enhancement of heat transfer using nanofluis – An overview. *Journal of Renewable and Sustainable Energy Reviews*. **14**, 629-641.

Jordan, A., R. Scholz, P. Wust, H. Fahling, and Felix, R. 1999. Magnetic fluid hyperthermia (MFH): cancer treatment with ac magnetic field induced excitation of biocompatible superparamagnetic nanoparticles. *J. Magn. Magn. Mater*., **201**(1–3): 413–419.

Jang, S.P. and Choi, S.U.S. 2004. Role of Brownian motion in the enhanced thermal conductivity of nanofluids. *Applieds Physics Letters*. **84**: 4316-8.

Maiga, S.E.B., Palm, S.J., Nguyen C.T., Roy, G. and Galanis, N. 2005. Heat Transfer enhancements by using nanofluids in forced convection flows. *International Journal of Heat and Fluid Flow*. **26**, 530 - 46.

Masuda, H., Ebata, A., Teramae, K. and Hishinuma, N., 1993. Alteration of thermal conductivity and viscosity of liquid by dispersing ultra fine particles. *Netsu Bussei*. **4**(4): 227–233

Maxwell, J.C. 1873. *Treatise on electricity and magnetism*. Oxford: Clarendon Press.

Maiga, S.E.B., Nguyen, C.T., Galanis, N., and Roy, G. 2003. Heat transfer behaviours of nanofluids in uniformly heated tube. Superlattices and Microsructures.

Mansour, R.B., Galanis, N., and Nguyen, C.T. 2007. Effect of uncertainties in physical properties on forced convection heat transfer with nanofluids. *Applied Thermal Engineering*. **27**(1): 240-9.

Murshed, S.M.S., Leong, K.C. and Yang, C.Y. 2008. Investigations of thermal conductivity and viscosity of nanofluids. *International Journal of Thermal Sciences*. **47**: 560-568

Pak, B.C. and Cho, I.Y. 1998. Hydrodynamic and heat transfer study of dispersed fluids with sub-micron metallic oxide particles. *Experimental Heat Transfer*. **11**: 151-70.

Sarma, P.K., Subramanyam, T., Kishore, P.S., Rao, V. D., Kakaç, S., 2002. A new method to predict convective heat transfer in a tube with twisted tape inserts for turbulent flow. *Int. J. Therm. Sci*. **41**, 955–960.

Sharma, K.V., Sundar, L.S. and Sarma, P.K. 2009. Estimation of heat transfer coefficient and friction factor in the transition flow with low volume concentration of Al2O3 nanofluid flowing in a circular tube and with twisted tape insert. *International Communications in Heat and Mass Transfer.* **36**: 503 – 507

Sundar, L. S., Ramanathan, S., Sharma, K.V. and Babu, P. S. 2007. Temperature Dependent Flow Charecteristics of Al_2O_3 Nanofluid. *International Journal of Nanotechnology and Applications* ISSN 0973-631X Volume **1** Number 2 pp. 35-44.

Sundar, L.S. and Sharma, K.V. 2010. Turbulent heat transfer and friction factor of Al2O3 Nanofluid in circular tube with twisted tape inserts. *International journal of Heat and Mass Transfer*. **53**: 1409-1416.

Taufid, M. 2010. *Simulation and Numerical Study of Nanofluid Forced Convection Heat Transfer*. Bach. Thesis. Universiti Malaysia Pahang, Malaysia.

Taufiq, M. 2010. *Development of the Regression Equation for Specific Heat and Density of Nanofluid*. Bach. Thesis. Universiti Malaysia Pahang, Malaysia.

Torii, S. 2009. Turbulent Heat Transfer behavior of nanofluid in a circular tube heated under constant heat flux. *Journal of Advance in Mechanical Engineering,* Article ID 917612.

Tufeu, R. 1990. Measurement of thermophysical properties of fluids. *Journal of Experimental Thermal and Fluid Sciences*. **3**:108-123

Tzeng, S.C., Lin, C.W., and Huang, K.D. 2005. Heat Transfer Enhancement of Nanofluids in Rotary Blade Coupling of Four Wheel Drive Vehicles. *Acta Mech*. **179**: pp. 80-91

Williams, W., Buongiorno, J., Hu, L.W. 2008. Experimental investigation of turbulent convective heat transfer and pressure loss of alumina/water and zirconia/water nanoparticle colloids (nanofluids) in horizontal tubes. *ASME Journal of Heat Transfer*. **130**:1–6.

Wang, X., Xu, X., Choi, S.U.S., 1999. Thermal conductivity of nanoparticle-fluid mixture. *Journal of Thermophysics and Heat Transfer*. **134**: 474-480

Xuan, Y., and Li, Q. 2003. Investigation on convective heat transfer and flow features of nanofluids. *Journal of Heat Transfer*, **125**: 151–155.

Xuan, Y., Li, Q., Jiang, J., Xu, and J. W. 2005. Experimental investigation on flow and convective heat transfer feature of a nanofluid for aerospace thermal management. *Journal of Astronautics.* **26**: 391-4.

Zhou, D.W. 2004. Heat transfer enhancement of copper nanofluid with acoustic cavitation. *International Journal of Heat and Mass Transfer*. **47:**3109-17.

APPENDIX A

STANDARD PROPERTIES OF WATER

TABLE A–9

Properties of saturated water

Temp. T, °C	Saturation Pressure P_{sat}, kPa	Density ρ, kg/m³		Enthalpy of Vaporization h_{fg}, kJ/kg	Specific Heat c_p, J/kg·K		Thermal Conductivity k, W/m·K		Dynamic Viscosity μ, kg/m·s		Prandtl Number Pr		Volume Expansion Coefficient β, 1/K
		Liquid	Vapor		Liquid	Vapor	Liquid	Vapor	Liquid	Vapor	Liquid	Vapor	Liquid
0.01	0.6113	999.8	0.0048	2501	4217	1854	0.561	0.0171	1.792×10^{-3}	0.922×10^{-5}	13.5	1.00	-0.068×10^{-3}
5	0.8721	999.9	0.0068	2490	4205	1857	0.571	0.0173	1.519×10^{-3}	0.934×10^{-5}	11.2	1.00	0.015×10^{-3}
10	1.2276	999.7	0.0094	2478	4194	1862	0.580	0.0176	1.307×10^{-3}	0.946×10^{-5}	9.45	1.00	0.733×10^{-3}
15	1.7051	999.1	0.0128	2466	4185	1863	0.589	0.0179	1.138×10^{-3}	0.959×10^{-5}	8.09	1.00	0.138×10^{-3}
20	2.339	998.0	0.0173	2454	4182	1867	0.598	0.0182	1.002×10^{-3}	0.973×10^{-5}	7.01	1.00	0.195×10^{-3}
25	3.169	997.0	0.0231	2442	4180	1870	0.607	0.0186	0.891×10^{-3}	0.987×10^{-5}	6.14	1.00	0.247×10^{-3}
30	4.246	996.0	0.0304	2431	4178	1875	0.615	0.0189	0.798×10^{-3}	1.001×10^{-5}	5.42	1.00	0.294×10^{-3}
35	5.628	994.0	0.0397	2419	4178	1880	0.623	0.0192	0.720×10^{-3}	1.016×10^{-5}	4.83	1.00	0.337×10^{-3}
40	7.384	992.1	0.0512	2407	4179	1885	0.631	0.0196	0.653×10^{-3}	1.031×10^{-5}	4.32	1.00	0.377×10^{-3}
45	9.593	990.1	0.0655	2395	4180	1892	0.637	0.0200	0.596×10^{-3}	1.046×10^{-5}	3.91	1.00	0.415×10^{-3}
50	12.35	988.1	0.0831	2383	4181	1900	0.644	0.0204	0.547×10^{-3}	1.062×10^{-5}	3.55	1.00	0.451×10^{-3}
55	15.76	985.2	0.1045	2371	4183	1908	0.649	0.0208	0.504×10^{-3}	1.077×10^{-5}	3.25	1.00	0.484×10^{-3}
60	19.94	983.3	0.1304	2359	4185	1916	0.654	0.0212	0.467×10^{-3}	1.093×10^{-5}	2.99	1.00	0.517×10^{-3}
65	25.03	980.4	0.1614	2346	4187	1926	0.659	0.0216	0.433×10^{-3}	1.110×10^{-5}	2.75	1.00	0.548×10^{-3}
70	31.19	977.5	0.1983	2334	4190	1936	0.663	0.0221	0.404×10^{-3}	1.126×10^{-5}	2.55	1.00	0.578×10^{-3}
75	38.58	974.7	0.2421	2321	4193	1948	0.667	0.0225	0.378×10^{-3}	1.142×10^{-5}	2.38	1.00	0.607×10^{-3}
80	47.39	971.8	0.2935	2309	4197	1962	0.670	0.0230	0.355×10^{-3}	1.159×10^{-5}	2.22	1.00	0.653×10^{-3}
85	57.83	968.1	0.3536	2296	4201	1977	0.673	0.0235	0.333×10^{-3}	1.176×10^{-5}	2.08	1.00	0.670×10^{-3}
90	70.14	965.3	0.4235	2283	4206	1993	0.675	0.0240	0.315×10^{-3}	1.193×10^{-5}	1.96	1.00	0.702×10^{-3}
95	84.55	961.5	0.5045	2270	4212	2010	0.677	0.0246	0.297×10^{-3}	1.210×10^{-5}	1.85	1.00	0.716×10^{-3}
100	101.33	957.9	0.5978	2257	4217	2029	0.679	0.0251	0.282×10^{-3}	1.227×10^{-5}	1.75	1.00	0.750×10^{-3}
110	143.27	950.6	0.8263	2230	4229	2071	0.682	0.0262	0.255×10^{-3}	1.261×10^{-5}	1.58	1.00	0.798×10^{-3}
120	198.53	943.4	1.121	2203	4244	2120	0.683	0.0275	0.232×10^{-3}	1.296×10^{-5}	1.44	1.00	0.858×10^{-3}
130	270.1	934.6	1.496	2174	4263	2177	0.684	0.0288	0.213×10^{-3}	1.330×10^{-5}	1.33	1.01	0.913×10^{-3}
140	361.3	921.7	1.965	2145	4286	2244	0.683	0.0301	0.197×10^{-3}	1.365×10^{-5}	1.24	1.02	0.970×10^{-3}
150	475.8	916.6	2.546	2114	4311	2314	0.682	0.0316	0.183×10^{-3}	1.399×10^{-5}	1.16	1.02	1.025×10^{-3}
160	617.8	907.4	3.256	2083	4340	2420	0.680	0.0331	0.170×10^{-3}	1.434×10^{-5}	1.09	1.05	1.145×10^{-3}
170	791.7	897.7	4.119	2050	4370	2490	0.677	0.0347	0.160×10^{-3}	1.468×10^{-5}	1.03	1.05	1.178×10^{-3}
180	1,002.1	887.3	5.153	2015	4410	2590	0.673	0.0364	0.150×10^{-3}	1.502×10^{-5}	0.983	1.07	1.210×10^{-3}
190	1,254.4	876.4	6.388	1979	4460	2710	0.669	0.0382	0.142×10^{-3}	1.537×10^{-5}	0.947	1.09	1.280×10^{-3}
200	1,553.8	864.3	7.852	1941	4500	2840	0.663	0.0401	0.134×10^{-3}	1.571×10^{-5}	0.910	1.11	1.350×10^{-3}
220	2,318	840.3	11.60	1859	4610	3110	0.650	0.0442	0.122×10^{-3}	1.641×10^{-5}	0.865	1.15	1.520×10^{-3}
240	3,344	813.7	16.73	1767	4760	3520	0.632	0.0487	0.111×10^{-3}	1.712×10^{-5}	0.836	1.24	1.720×10^{-3}
260	4,688	783.7	23.69	1663	4970	4070	0.609	0.0540	0.102×10^{-3}	1.788×10^{-5}	0.832	1.35	2.000×10^{-3}
280	6,412	750.8	33.15	1544	5280	4835	0.581	0.0605	0.094×10^{-3}	1.870×10^{-5}	0.854	1.49	2.380×10^{-3}
300	8,581	713.8	46.15	1405	5750	5980	0.548	0.0695	0.086×10^{-3}	1.965×10^{-5}	0.902	1.69	2.950×10^{-3}
320	11,274	667.1	64.57	1239	6540	7900	0.509	0.0836	0.078×10^{-3}	2.084×10^{-5}	1.00	1.97	
340	14,586	610.5	92.62	1028	8240	11,870	0.469	0.110	0.070×10^{-3}	2.255×10^{-5}	1.23	2.43	
360	18,651	528.3	144.0	720	14,690	25,800	0.427	0.178	0.060×10^{-3}	2.571×10^{-5}	2.06	3.73	
374.14	22,090	317.0	317.0	0	—	—	—	—	0.043×10^{-3}	4.313×10^{-5}			

Note 1: Kinematic viscosity ν and thermal diffusivity α can be calculated from their definitions, $\nu = \mu/\rho$ and $\alpha = k/\rho c_p = \nu/\text{Pr}$. The temperatures 0.01°C, 100°C, and 374.14°C are the triple-, boiling-, and critical-point temperatures of water, respectively. The properties listed above (except the vapor density) can be used at any pressure with negligible error except at temperatures near the critical-point value.

Note 2: The unit kJ/kg · °C for specific heat is equivalent to kJ/kg · K, and the unit W/m · °C for thermal conductivity is equivalent to W/m · K.

Source: Viscosity and thermal conductivity data are from J. V. Sengers and J. T. R. Watson, *Journal of Physical and Chemical Reference Data* 15 (1986), pp. 1291–1322. Other data are obtained from various sources or calculated.

Source: Cengel (2006)

APPENDIX B1

DATA FROM EXPERIMENT

Table 6.1: Data distributions for experiment by water

Run	Ø (%)	$\dot{m}$, (Kg/s)	Avg. T_w (°C)	T_b (°C)	Re	h_{exp} (W/m^2.K) (Crude)	Nu_{exp} (crude)	h_{exp} (W/m^2.K) (True)	Nu_{exp} (True)
1	0	0.03647	72.96	39.70	3787.93	191.41	5.77	1000.11	30.17
2	0	0.04638	70.96	38.35	4682.87	195.22	5.91	1149.34	34.78
3	0	0.05641	69.00	37.45	5587.42	201.78	6.12	1300.59	39.44
4	0	0.06573	67.03	36.35	6357.69	207.50	6.31	1429.74	43.47
5	0	0.07630	65.43	35.45	7236.10	212.35	6.47	1562.83	47.62
6	0	0.08966	62.83	34.90	8400.45	227.93	6.95	1740.67	53.11
7	0	0.10445	67.26	37.65	10390.18	215.00	6.52	2356.29	71.42
8	0	0.12726	62.63	36.95	12470.26	247.90	7.53	2679.13	81.34
9	0	0.14325	59.89	36.50	13901.02	272.18	8.27	2909.86	88.44
10	0	0.16256	56.58	35.35	15382.87	299.87	9.14	3183.63	97.03
11	0	0.18886	52.42	33.20	17036.53	331.23	10.15	3502.59	107.32
12	0	0.22495	48.92	31.25	19404.75	360.28	11.09	3773.65	116.20

Table 6.2: Properties of water determine by Azmi et al. (2010) equations

Run	T_b (°C)	Prandtl Number Pr	Density ρ (kg/m^3)	Specific Heat, Cp (J/kg. K)	Thermal Conductivity k, (W/m.K)	Dynamic Viscosity μ, (kg/m.s)
1	39.70	4.2802	992.363	4178.294	0.6298	0.000645
2	38.35	4.4166	992.869	4178.132	0.6279	0.000664
3	37.45	4.5115	993.199	4178.047	0.6266	0.000677
4	36.35	4.6320	993.593	4177.972	0.6249	0.000693
5	35.45	4.7344	993.908	4177.935	0.6236	0.000707

Table 6.2: Continued

Run	T_b (ºC)	Prandtl Number Pr	Density ρ (kg/m³)	Specific Heat, Cp (J/kg. K)	Thermal Conductivity k, (W/m.K)	Dynamic Viscosity μ, (kg/m.s)
6	34.90	4.7987	994.098	4177.924	0.6227	0.000715
7	37.65	4.4901	993.126	4178.064	0.6268	0.000674
8	36.95	4.5656	993.379	4178.009	0.6258	0.000684
9	36.50	4.6152	993.539	4177.981	0.6251	0.000691
10	35.35	4.7460	993.943	4177.932	0.6234	0.000708
11	33.20	5.0059	994.668	4177.946	0.6201	0.000743
12	31.25	5.2602	995.293	4178.091	0.6170	0.000777

APPENDIX B2

DATA FROM EXPERIMENT

Table 6.3: Data distributions for experiment by Al_2O_3/Water with 0.02% concentration

Run	Ø (%)	$\dot{m}$, (Kg/s)	Avg. T_w (°C)	T_b (°C)	Re	h_{exp} (W/$m^2.K$) (Crude)	Nu_{exp} (crude)	h_{exp} (W/$m^2.K$) (True)	Nu_{exp} (True)
					V = 190V & I = 3 A				
1	0.02	0.03647	71.40	39.95	3593.50	202.42	31.11	1090.62	29.78
2	0.02	0.04638	68.56	38.50	4426.94	211.78	36.01	1290.94	35.55
3	0.02	0.05641	66.56	37.55	5271.13	219.45	40.81	1463.60	40.53
4	0.02	0.06573	64.50	36.45	6049.46	226.96	45.41	1633.58	45.53
5	0.02	0.07630	62.70	35.55	6815.57	234.48	49.68	1800.39	50.45
6	0.02	0.08966	61.00	35.05	8203.41	245.33	57.33	2022.34	56.84
7	0.02	0.10445	65.66	37.65	9699.70	227.28	71.57	2496.12	69.07
8	0.02	0.12726	61.02	37.00	11671.89	265.04	82.64	2910.06	80.84
9	0.02	0.14325	58.48	36.65	13044.94	291.63	90.80	3201.00	89.11
10	0.02	0.16256	55.00	35.50	14385.42	326.47	93.65	3345.34	93.77
11	0.02	0.18886	50.75	33.25	15852.02	363.78	108.08	3874.09	110.08
12	0.02	0.22495	47.46	31.40	17754.62	396.40	120.47	4304.53	123.71

Table 6.4: Properties of Al_2O_3/Water with 0.02% concentration determine by Azmi et al. (2010) and Taufiq equations

Run	T_b (°C)	Prandtl Number Pr	Density ρ (kg/m^3)	Specific Heat, Cp (J/kg. K)	Thermal Conductivity k, (W/m.K)	Dynamic Viscosity μ, (kg/m.s)
1	39.95	4.0763	993.024	4168.573	0.6959	0.000680
2	38.50	4.2440	993.525	4168.297	0.6900	0.000703
3	37.55	4.3594	993.844	4168.142	0.6862	0.000718
4	36.45	4.4987	994.204	4167.991	0.6817	0.000736

Table 6.4: Continued

Run	T_b (°C)	Prandtl Number Pr	Density ρ (kg/m^3)	Specific Heat, Cp $(J/kg.\ K)$	Thermal Conductivity $k,\ (W/m.K)$	Dynamic Viscosity $\mu,\ (kg/m.s)$
5	35.55	4.6174	994.492	4167.892	0.6781	0.000751
6	35.05	4.6853	994.650	4167.847	0.6760	0.000760
7	37.65	4.3470	993.811	4168.157	0.6866	0.000716
8	37.00	4.4283	994.025	4168.063	0.6840	0.000727
9	36.65	4.4729	994.140	4168.016	0.6825	0.000732
10	35.50	4.6242	994.508	4167.887	0.6779	0.000752
11	33.25	4.9412	995.199	4167.746	0.6687	0.000793
12	31.40	5.2242	995.735	4167.753	0.6611	0.000829

APPENDIX B3

DATA FROM EXPERIMENT

Table 6.5: Data distributions for experiment by Al_2O_3/Water with 0.10% concentration

Run	Ø (%)	$\dot{m}$, (Kg/s)	Avg. T_w (°C)	T_b (°C)	Re	h_{exp} (W/$m^2.K$) (Crude)	Nu_{exp} (crude)	h_{exp} (W/$m^2.K$) (True)	Nu_{exp} (True)
					V = 190V & I = 3 A				
1	0.1	0.036585	69.33	40.10	3581.00	217.80	31.06	1171.56	31.93
2	0.1	0.049916	66.43	38.60	4727.42	228.75	37.63	1457.11	40.06
3	0.1	0.056572	64.93	37.65	5245.19	233.37	40.69	1551.84	42.90
4	0.1	0.069965	62.66	36.55	6327.21	243.82	46.72	1805.59	50.24
5	0.1	0.079989	59.90	35.65	7085.82	262.52	50.98	2068.44	57.86
6	0.1	0.093225	58.56	35.15	7788.73	250.54	58.85	2120.08	60.21
7	0.1	0.121416	58.33	38.05	11358.84	313.92	60.28	2903.70	80.08
8	0.1	0.153023	56.76	37.45	14124.05	329.68	75.60	3311.49	91.65
9	0.1	0.169757	55.26	36.95	15492.26	347.69	86.58	3639.00	101.01
10	0.1	0.182826	53.36	35.95	16307.95	365.66	98.54	3942.58	110.09
11	0.1	0.213267	49.93	33.65	18030.16	391.04	106.41	4100.06	116.09
12	0.1	0.243398	47.53	31.75	19665.80	403.43	123.06	4475.09	128.19

Table 6.6: Properties of Al_2O_3/Water with 0.10% concentration determine by Azmi et al. (2010) and Taufiq equations

Run	T_b (°C)	Prandtl Number Pr	Density ρ (kg/m^3)	Specific Heat, Cp (J/kg. K)	Thermal Conductivity k, (W/m.K)	Dynamic Viscosity μ, (kg/m.s)
1	40.10	4.0824	995.738	4157.426	0.6972	0.000685
2	38.60	4.2559	996.259	4157.137	0.6912	0.000708
3	37.65	4.3714	996.579	4156.980	0.6873	0.000723
4	36.55	4.5109	996.942	4156.827	0.6828	0.000741

Table 6.6: Continued

Run	T_b (°C)	Prandtl Number Pr	Density ρ (kg/m³)	Specific Heat, Cp (J/kg. K)	Thermal Conductivity k, (W/m.K)	Dynamic Viscosity μ, (kg/m.s)
5	35.65	4.6298	997.232	4156.725	0.6792	0.000756
6	35.15	4.9835	998.002	4156.566	0.6690	0.000802
7	38.05	4.3223	996.445	4157.043	0.6889	0.000716
8	37.45	4.3963	996.646	4156.950	0.6865	0.000726
9	36.95	4.4595	996.811	4156.879	0.6845	0.000734
10	35.95	4.5897	997.136	4156.757	0.6804	0.000751
11	33.65	4.9099	997.852	4156.583	0.6710	0.000793
12	31.75	5.1977	998.410	4156.565	0.6633	0.000829

APPENDIX B4

DATA FROM EXPERIMENT

Table 6.7: Data distributions for experiment by Al_2O_3/Water with 0.50% concentration

						V = 190V & I = 3 A				
Run	$\emptyset$ (%)	$\dot{m},$ (Kg/s)	Avg. T_w (°C)	T_b (°C)	Re	h_{exp} (W/m^2.K) (Crude)	Nu_{exp} (crude)	h_{exp} (W/m^2.K) (True)	Nu_{exp} (True)
1	0.5	0.037026	68.10	40.25	3474.25	228.59	30.80	1219.32	33.03
2	0.5	0.047134	65.23	38.58	4263.84	238.88	36.09	1459.35	39.92
3	0.5	0.057188	63.16	37.85	5089.88	251.53	40.28	1655.77	45.48
4	0.5	0.070745	60.96	36.75	6142.18	262.96	46.19	1925.20	53.23
5	0.5	0.080872	59.06	35.85	6878.51	274.29	50.39	2136.11	59.38
6	0.5	0.097726	57.83	35.35	8216.79	283.19	57.81	2354.06	65.63
7	0.5	0.122856	57.56	38.20	11020.33	328.83	58.11	2932.19	80.38
8	0.5	0.154904	56.10	37.60	13709.76	344.12	74.35	3399.33	93.51
9	0.5	0.171804	54.76	37.05	15018.07	359.47	85.07	3696.67	102.02
10	0.5	0.184988	52.76	36.05	15806.40	380.98	88.67	3696.30	102.62
11	0.5	0.215749	49.46	33.70	17454.93	403.95	104.38	4154.54	116.98
12	0.5	0.246199	47.20	31.90	19083.92	416.09	120.78	4529.97	128.96

Table 6.8: Properties of Al_2O_3/Water with 0.50% concentration determine by Azmi et al. (2010) and Taufiq equations

Run	T_b (°C)	Prandtl Number Pr	Density ρ (kg/m^3)	Specific Heat, Cp (J/kg. K)	Thermal Conductivity k, (W/m.K)	Dynamic Viscosity μ, (kg/m.s)
1	40.25	4.1763	1009.515	4101.568	0.7014	0.000714
2	38.58	4.3737	1010.105	4101.246	0.6946	0.000741
3	37.85	4.4643	1010.356	4101.125	0.6917	0.000753
4	36.75	4.6060	1010.725	4100.967	0.6872	0.000772

Table 6.8: Continued

Run	T_b (°C)	Prandtl Number Pr	Density ρ (kg/m^3)	Specific Heat, Cp $(J/kg.\ K)$	Thermal Conductivity $k,\ (W/m.K)$	Dynamic Viscosity $\mu,\ (kg/m.s)$
5	35.85	4.7268	1011.021	4100.862	0.6835	0.000788
6	35.35	4.7958	1011.182	4100.812	0.6815	0.000797
7	38.20	4.4205	1010.236	4101.182	0.6931	0.000747
8	37.60	4.4959	1010.441	4101.087	0.6907	0.000757
9	37.05	4.5667	1010.626	4101.007	0.6884	0.000767
10	36.05	4.6996	1010.956	4100.883	0.6844	0.000784
11	33.70	5.0338	1011.700	4100.701	0.6748	0.000828
12	31.90	5.3119	1012.239	4100.677	0.6674	0.000865

APPENDIX C

SAMPLE OF CALCULATION

Sample calculation of heat transfer coefficient, h and Nusselt number, Nu for water and nanofluid with 0.02% volume concentrations.

i. HTC Predicion by using Gnielinski Eq.

From Eq. 2.25

$$Re = \frac{4\dot{m}}{\pi D_i \mu}$$

$$= \frac{4\,(0.03647\,\frac{kg}{s})}{\pi(0.019\,m)(0.000645\,\frac{kg}{m.s})}$$

$$= 3787.93$$

From Eq. 2.26

$$Pr = \frac{\textit{Molekular diffusivity of momentum}}{\textit{Molekular diffusivity of heat}} = \frac{v}{\alpha} = \frac{\mu C_p}{k}$$

$$= \frac{0.000645\,\frac{kg}{m.s} \times 4178.29\,\frac{J}{kg.K}}{0.6298\,\frac{W}{m.K}}$$

$$= 4.2802$$

From Eq. 2.20

$$f = (1.58 \ln Re - 3.82)^{-2}$$

$$= (1.58\, ln(3787.93) - 3.82)^{-2}$$

$$= 0.0118$$

From Eq. 2.19

$$Nu = \frac{\left(\frac{f}{2}\right)(Re - 1000)Pr}{1 + 12.7\left(\frac{f}{2}\right)^{0.5}\left(Pr^{\frac{2}{3}} - 1\right)}$$

$$= \frac{\frac{0.0118}{2}(3787.93 - 1000)(4.2802)}{1 + 12.7\left(\frac{0.0118}{2}\right)^{0.5}\left(4.2802^{\frac{2}{3}} - 1\right)}$$

$$= 27.15$$

From Eq. 2.18

$$Nu = \frac{hD}{k} \quad ; \quad h = \frac{Nuk}{D}$$

$$= \frac{27.15 \times 0.6298\frac{W}{m.K}}{0.019m}$$

$$= 899.95\,\frac{W}{m^2.K}$$

ii.   HTC Experiment (Water)

$T_b = 39.7\ ^oC$; $T_w = 72.96\ ^oC$; $V = 190$ Volt ; $I = 3$ A

$$A_s = \pi DL = \pi(0.019m)(1.5m)$$

$$= 0.089535m^2$$

From Eq. 2.1

$$\dot{Q} = V \times I = hA_s(T_w - T_b)_{avg}$$

$$h_{w,\ exp.\ (Crude)} = \frac{V \times I}{A_s(T_w - T_b)_{avg}}$$

$$= \frac{190V \times 3\ Amphere}{0.089535m^2(72.96 - 39.7)°C}$$

$$= 191.41\frac{W}{m^2.K}$$

$$Nu_{w,\ exp.\ (Crude)} = \frac{h_{w,\ exp.\ (Crude)}D}{k}$$

$$= \frac{191.41\frac{W}{m^2.K}(0.019m)}{0.6298\frac{W}{m.K}}$$

$$= 5.77$$

$$\frac{h_{w,\ exp(Crude)}}{h_{w,\ theory}} = \frac{Nu_{w,\ exp(Crude)}}{Nu_{w,\ theory}}$$

$$h_{w,\ theory} = h_{w.exp(True\ Value)} = h_{w,\ exp(Crude)} \times \left(\frac{Nu_{w,\ theory}}{Nu_{w,\ exp(Crude)}} \right)$$

$$= 191.41 \frac{W}{m^2.K} \times \left(\frac{30.17}{5.77} \right)$$

$$= 1000.11 \frac{W}{m^2.K}$$

$$Nu_{exp,\ new(True\ Value)} = \frac{h_{theory,\ water} D}{k}$$

$$= \frac{1000.11 \frac{W}{m^2.K} (0.019m)}{0.6298 \frac{W}{m.K}}$$

$$= 30.17$$

iii. Actual HTC for Al_2O_3/Water with $\emptyset = 0.02\%$

$T_b = 39.95\ ^{\circ}C$; $T_w = 71.40\ ^{\circ}C$; $V = 190$ Volt ; $I = 3$ A

$$A_s = \pi DL = \pi(0.019m)(1.5m)$$

$$= 0.089535m^2$$

$$\dot{Q} = V \times I = hA_s(T_w - T_b)_{avg}$$

$$h_{nf, exp.\ (Crude)} = \frac{V \times I}{A_s(T_w - T_b)_{avg}}$$

$$= \frac{190\ V \times 3\ Amphere}{0.089535\text{m}^2(71.40 - 39.95)°C}$$

$$= 202.42\ \frac{W}{m^2.K}$$

$$\frac{h_{nf,\ exp(Crude)}}{h_{nf,\ theory}} = \frac{Nu_{w,\ exp(Crude)}}{Nu_{w,\ theory}}$$

$$h_{nf,\ theory} = h_{nf.theory(True\ Value)} = h_{nf,\ exp} \times \left(\frac{Nu_{theory,\ water}}{Nu_{exp,\ water}}\right)$$

$$= 202.42\ \frac{W}{m^2.K} \times \left(\frac{31.11}{5.77}\right)$$

$$= 1090.62\ \frac{W}{m^2.K}$$

$$Nu_{nf,\ exp(\ True\ Value)} = \frac{h_{nf,\ theory(True\ Value)}D}{k}$$

$$= \frac{1090.62\ \frac{W}{m^2.K}(0.019m)}{0.69588\ \frac{W}{m^2.K}}$$

$$= 29.78$$

APPENDIX D

DATA FROM NUMERICAL STUDY BY TAUFID, (2010)

Table 6.9: Data distribution from numerical study of water

Run	$\emptyset$ (%)	$\dot{m}$ (kg/s)	T_w (˚C)	T_b (˚C)	Pr	Re	h_{sim} (W/m²·K)	Nu_{sim}
1	0	0.03647	69.47	37.78	4.4767	3637.63	1088.95	33.00
2	0	0.04638	66.17	35.65	4.7115	4417.75	1210.28	36.86
3	0	0.05641	63.90	34.85	4.8040	5279.87	1407.86	42.96
4	0	0.06573	62.34	34.31	4.8693	6077.93	1586.04	48.46
5	0	0.0763	60.96	33.28	4.9962	6893.81	1658.28	50.80
6	0	0.08966	59.63	32.88	5.0465	8028.15	1887.41	57.88
7	0	0.10445	58.50	32.54	5.0895	9281.39	2136.02	65.56
8	0	0.12726	57.24	32.17	5.1385	11211.15	2508.31	77.06
9	0	0.14325	56.58	31.97	5.1646	12562.51	2761.79	84.89
10	0	0.16256	55.94	31.78	5.1899	14193.53	3058.90	94.06
11	0	0.18886	55.26	31.57	5.2167	16413.68	3450.14	106.15
12	0	0.22495	54.58	31.14	5.2751	19355.50	3702.06	114.03

Table 6.10: Data contribution from numerical study of Alumina with $\emptyset = 0.02\%$

Run	$\emptyset$ (%)	$\dot{m}$ (kg/s)	T_w (˚C)	T_b (˚C)	Pr	Re	h_{sim} (W/m²·K)	Nu_{sim}
1	0.02	0.03647	68.57	38.42	4.2419	3480.80	1255.07	34.58
2	0.02	0.04638	65.27	36.04	4.5403	4194.38	1380.14	38.57
3	0.02	0.05641	63.69	35.60	4.5988	5049.92	1574.58	44.12
4	0.02	0.06573	62.01	34.88	4.6964	5786.94	1787.49	50.30
5	0.02	0.0763	60.40	33.63	4.8743	6522.03	1880.58	53.33
6	0.02	0.08966	59.08	33.13	4.9463	7575.32	2143.06	60.95
7	0.02	0.10445	58.30	32.86	4.9873	8767.26	2337.91	66.61
8	0.02	0.12726	56.93	32.29	5.0731	10538.03	2743.69	78.44
9	0.02	0.14325	56.28	32.06	5.1083	11796.97	3020.42	86.47
10	0.02	0.16256	55.68	31.87	5.1380	13325.78	3343.90	95.85
11	0.02	0.18886	55.06	31.68	5.1679	15410.47	3760.71	107.92
12	0.02	0.22495	54.38	31.19	5.2445	18141.79	3998.23	115.08

Table 6.11: Data contribution from numerical study of Alumina with $\emptyset = 0.10\%$

Run	$\emptyset$ (%)	$\dot{m}$ (kg/s)	T_w (°C)	T_b (°C)	Pr	Re	h_{sim} (W/m^2.K)	Nu_{sim}
1	0.1	0.036585	68.48	39.17	4.1540	3549.97	1368.38	37.54
2	0.1	0.049916	64.98	36.53	4.4768	4564.70	1507.43	42.00
3	0.1	0.056572	63.58	35.99	4.5474	5109.56	1678.14	46.91
4	0.1	0.069965	61.95	35.17	4.6572	6200.62	1879.02	52.78
5	0.1	0.079989	60.30	33.82	4.8463	6868.38	1966.15	55.69
6	0.1	0.093225	59.00	33.29	4.9233	7905.33	2231.98	63.42
7	0.1	0.121416	58.24	33.04	4.9607	10234.15	2449.92	69.72
8	0.1	0.153023	56.87	32.39	5.0581	12700.50	2840.83	81.16
9	0.1	0.169757	56.22	32.14	5.0963	14005.36	3123.17	89.37
10	0.1	0.182826	55.62	31.95	5.1259	15014.44	3470.29	99.42
11	0.1	0.213267	55.01	31.76	5.1557	17433.84	3921.33	112.47
12	0.1	0.243398	54.32	31.27	5.2321	19665.67	4180.27	120.26

Table 6.12: Data contribution from numerical study of Alumina with $\emptyset = 0.50\%$

Run	$\emptyset$ (%)	$\dot{m}$ (kg/s)	T_w (°C)	T_b (°C)	Pr	Re	h_{sim} (W/m^2.K)	Nu_{sim}
1	0.5	0.03703	68.29	39.75	4.0890	3636.99	1491.21	41.07
2	0.5	0.04713	64.79	36.61	4.4680	4315.94	1556.36	43.54
3	0.5	0.05719	63.39	36.07	4.5384	5172.03	1739.00	48.88
4	0.5	0.07075	61.76	35.25	4.6479	6278.15	1955.65	55.15
5	0.5	0.08087	60.11	33.90	4.8365	6953.72	2050.22	58.18
6	0.5	0.09773	58.81	33.37	4.9133	8298.45	2340.94	66.59
7	0.5	0.12286	58.05	33.12	4.9506	10369.87	2581.83	73.60
8	0.5	0.15490	56.69	32.47	5.0477	12874.60	3019.74	86.28
9	0.5	0.17180	56.03	32.22	5.0858	14194.12	3340.76	95.57
10	0.5	0.18499	55.51	32.03	5.1152	15213.36	3655.12	104.68
11	0.5	0.21575	54.92	31.83	5.1461	17658.63	4113.29	117.95
12	0.5	0.24620	54.27	31.29	5.2307	19891.31	4272.19	122.88

APPENDIX E1

GANTT CHART

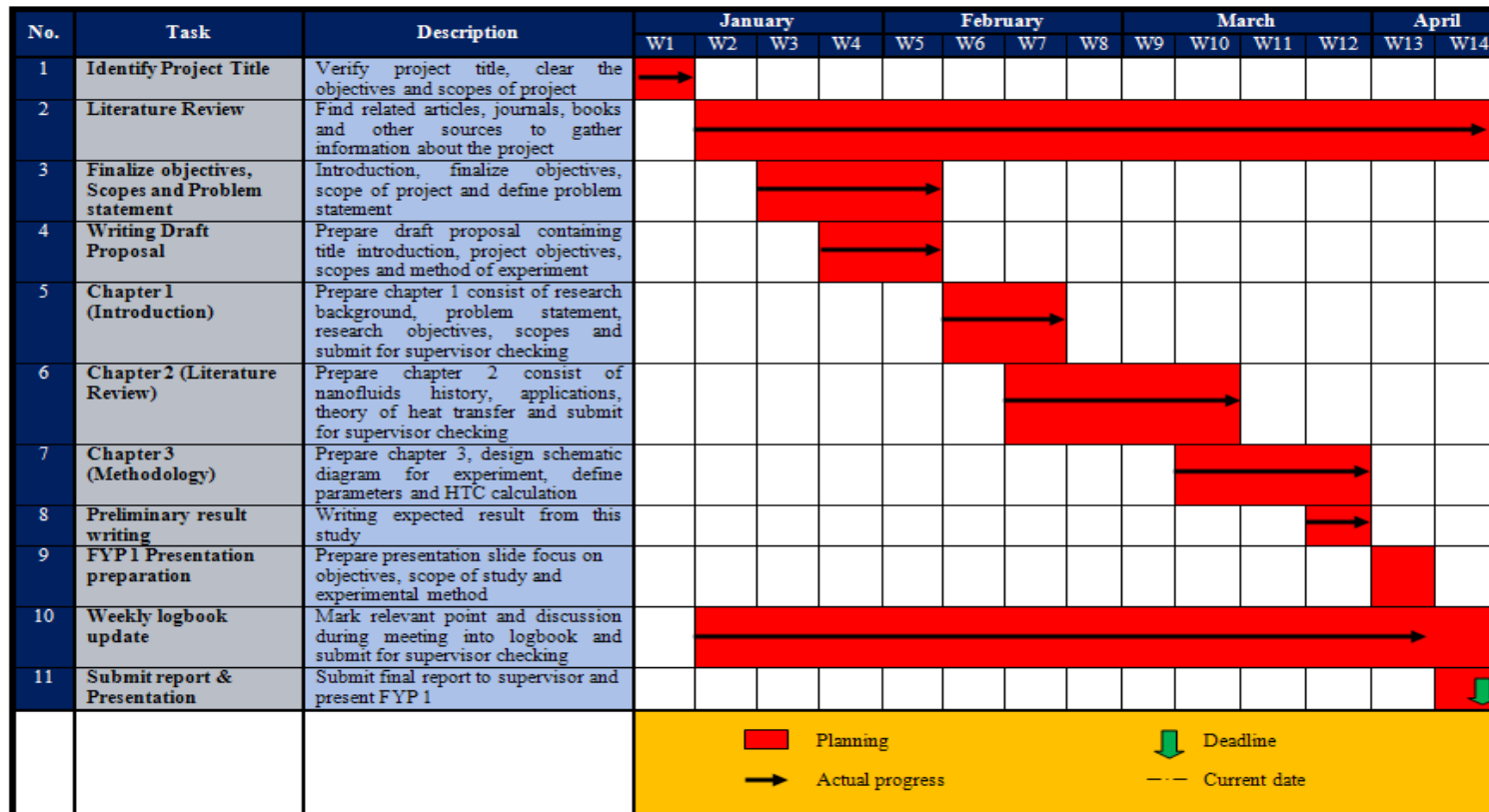| No.	Task	Description	January				February				March				April	
			W1	W2	W3	W4	W5	W6	W7	W8	W9	W10	W11	W12	W13	W14
1	Identify Project Title	Verify project title, clear the objectives and scopes of project	→													
2	Literature Review	Find related articles, journals, books and other sources to gather information about the project		→												
3	Finalize objectives, Scopes and Problem statement	Introduction, finalize objectives, scope of project and define problem statement			→											
4	Writing Draft Proposal	Prepare draft proposal containing title introduction, project objectives, scopes and method of experiment				→										
5	Chapter 1 (Introduction)	Prepare chapter 1 consist of research background, problem statement, research objectives, scopes and submit for supervisor checking						→								
6	Chapter 2 (Literature Review)	Prepare chapter 2 consist of nanofluids history, applications, theory of heat transfer and submit for supervisor checking								→						
7	Chapter 3 (Methodology)	Prepare chapter 3, design schematic diagram for experiment, define parameters and HTC calculation											→			
8	Preliminary result writing	Writing expected result from this study												→		
9	FYP 1 Presentation preparation	Prepare presentation slide focus on objectives, scope of study and experimental method													→	
10	Weekly logbook update	Mark relevant point and discussion during meeting into logbook and submit for supervisor checking		→												
11	Submit report & Presentation	Submit final report to supervisor and present FYP 1														⬇
			▇ Planning								⬇ Deadline					
			→ Actual progress								— · — Current date					

Figure 6.1: Gantt chart for FYP 1

APPENDIX E2

GANTT CHART

No.	Task	Description	July				August				September				Oct/Nov		
			W1	W2	W3	W4	W5	W6	W7	W8	W9	W10	W11	W12	W13	W14	W15
1	Experiment	Sample preparation, calibrate apparatus, Running experiment, collect data and validate	■	■	■	■				→							
2	Confirming data	Determine HTC and discuss with supervisor or validate with result from numerical and previous study					■	■			→						
3	Combine result and Discussion	Discuss result and writing discussion and relationship of HTC with parameters considered							■	■	■			→			
4	Writing Conclusion and Recommendation	Prepare conclusion and recommendation for improvement based on this experiment result											■	■	→		
5	Final report draft submission	Submit final report draft consist of all chapters, references, appendices, abbreviation and table of content for checking													■	→	
6	Preparation for FYP 2 presentation	Focus on result obtain from experiment either it achieved the objectives of the study or not													■	→	
7	Weekly logbook update	Mark relevant point and discussion during meeting into logbook and submit for supervisor checking	■	■	■	■	■	■	■	■	■	■	■	■	■	→	
8	FYP2 Presentation	Present the result found from this study														■	→
9	Final report submission and documented	Submit the final report and study is successfully finish															↓
			■ Planning **↓ Deadline**														
			→ Actual progress **—·— Current date**														

Figure 6.2: Gantt chart for FYP 2

APPENDIX F

NANOFLUID PREPARATION

Figure	Description
	Al_2O_3 Nanoparticles
	Nanoparticles is weighted before dispersed in water

Figure	Description

Weighing of nanoparticles

Stirrer of nanofluid

Sample of nanofluids after stirrer